cmgh
CELLULAR AND MOLECULAR GASTROENTEROLOGY AND HEPATOLOGY

ORIGINAL RESEARCH

Hepatitis B Virus Utilizes a Retrograde Trafficking Route via the Trans-Golgi Network to Avoid Lysosomal Degradation

Ying-Yi Li,[1,*] Kazuyuki Kuroki,[1] Tetsuro Shimakami,[1] Kazuhisa Murai,[2] Kazunori Kawaguchi,[1] Takayoshi Shirasaki,[2] Kouki Nio,[1] Saiho Sugimoto,[1] Tomoki Nishikawa,[1] Hikari Okada,[1] Noriaki Orita,[1] Hideo Takayama,[1] Ying Wang,[2] Phuong Doan Thi Bich,[1] Astuya Ishida,[1] Sadahiro Iwabuchi,[3] Shinichi Hashimoto,[3] Takeshi Shimaoka,[4] Noriko Tabata,[5] Miho Watanabe-Takahashi,[6] Kiyotaka Nishikawa,[6] Hiroshi Yanagawa,[5] Motoharu Seiki,[1] Kouji Matsushima,[4] Taro Yamashita,[1] Shuichi Kaneko,[1] and Masao Honda[1,2,*]

[1]Department of Gastroenterology, Kanazawa University Graduate School of Medicine, Kanazawa, Japan; [2]Department of Clinical Laboratory Medicine, Kanazawa University Graduate School of Health Medicine, Kanazawa, Japan; [3]Department of Molecular Pathophysiology, Institute of Advanced Medicine, Wakayama Medical University, Wakayama, Japan; [4]Division of Molecular Regulation of Inflammatory and Immune Diseases, Research Institute for Biomedical Sciences, Tokyo University of Science, Chiba, Japan; [5]Purotech Bio Inc, Kanagawa, Japan; and [6]Department of Molecular Life Sciences, Doshisha University, Kyoto, Japan

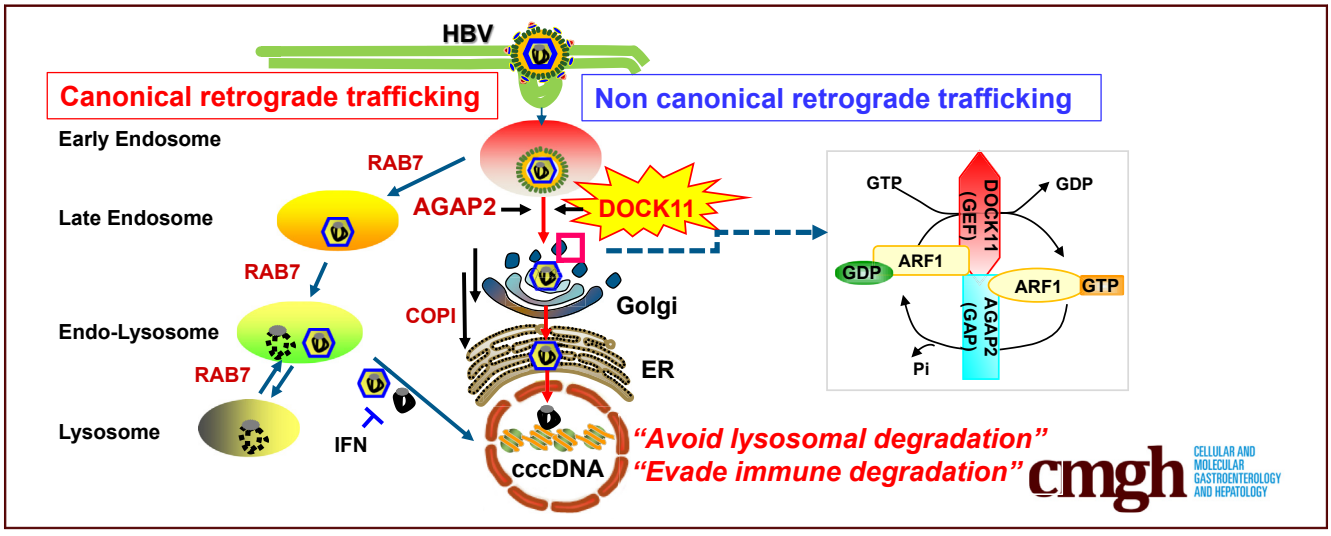

SUMMARY

We reveal that HBV uses a retrograde trafficking route via the trans-Golgi network and endoplasmic reticulum to enter into the nucleus of hepatocytes, thereby avoiding lysosomal degradation. DOCK11 contributes to HBV retrograde trafficking to maintain cccDNA levels. Thus, targeting DOCK11 may be a viable anti-HBV strategy.

BACKGROUND & AIMS: Hepatitis B virus (HBV) infection is difficult to cure owing to the persistence of covalently closed circular viral DNA (cccDNA). We performed single-cell transcriptome analysis of newly established HBV-positive and HBV-negative hepatocellular carcinoma cell lines and found that dedicator of cytokinesis 11 (DOCK11) was crucially involved in HBV persistence. However, the roles of DOCK11 in the HBV lifecycle have not been clarified.

METHODS: The cccDNA levels were measured by Southern blotting and real-time detection polymerase chain reaction in various hepatocytes including PXB cells by using an HBV-infected model. The retrograde trafficking route of HBV capsid was investigated by super-resolution microscopy, proximity ligation assay, and time-lapse analysis. The downstream molecules of DOCK11 and underlying mechanism were examined by liquid chromatography-tandem mass spectrometry, immunoblotting, and enzyme-linked immunosorbent assay.

RESULTS: The cccDNA levels were strongly increased by DOCK11 overexpression and repressed by DOCK11 suppression. Interestingly, DOCK11 functionally associated with retrograde trafficking proteins in the trans-Golgi network (TGN), Arf-GAP with GTPase domain, ankyrin repeat, and pleckstrin homology domain-containing protein 2 (AGAP2), and ADP-ribosylation factor 1 (ARF1), together with HBV capsid, to open an alternative retrograde trafficking route for

HBV from early endosomes (EEs) to the TGN and then to the endoplasmic reticulum (ER), thereby avoiding lysosomal degradation. Clinically, DOCK11 levels in liver biopsies from patients with chronic hepatitis B were significantly reduced by entecavir treatment, and this reduction correlated with HBV surface antigen levels.

CONCLUSIONS: HBV uses a retrograde trafficking route via EEs-TGN-ER for infection that is facilitated by DOCK11 and serves to maintain cccDNA. Therefore, DOCK11 is a potential therapeutic target to prevent persistent HBV infection. *(Cell Mol Gastroenterol Hepatol 2023;15:533–558; https://doi.org/10.1016/j.jcmgh.2022.10.008)*

Keywords: cccDNA; DOCK11; Retrograde Trafficking; AGAP2.

Chronic hepatitis B virus (HBV) infection greatly increases the risk of liver fibrosis, cirrhosis, and hepatocellular carcinoma (HCC) and is responsible for nearly 1 million annual deaths worldwide.[1] Current therapies rarely achieve a cure because they do not eliminate covalently closed circular viral DNA (cccDNA), which is responsible for viral persistence. Understanding the fundamental molecular mechanisms governing cccDNA biogenesis is essential for the development of new anti-HBV drugs.

In an effort to elucidate the host factors required for HBV maintenance, we established a new HCC cell line (named HC1) derived from a patient with chronic hepatitis B (CHB). We identified the host factors that were differentially upregulated in HBV-positive HC1 cells compared with HBV-negative HC1 cells using single-cell transcriptome analysis.[2] One of the identified host factors was dedicator of cytokinesis 11 (DOCK11).[3]

DOCK11 was originally cloned as the proto-oncogene CT10 regulator of kinase-binding protein and is highly expressed in placenta, lung, kidney, pancreas, and ovary.[4] DOCK11$^{-/-}$ mice show no critical phenotype of viability, fertility, or malformation and have a normal germinal center response.[5] DOCK11 is a specific guanine nucleotide exchange factor (GEF) for cell division cycle 42 (CDC42), with its GEF activity originating from the DOCK homology region 2 (DHR2) domain.[6] CDC42 is the only identified partner of DOCK11 and has a role in the establishment of cell polarity.[7] However, the roles of DOCK11 in the HBV life cycle have not been clarified.

The discovery of the HBV receptor Na/taurocholate cotransporting polypeptide (NTCP) clarified the initial step of HBV infection from the cell surface to the cytoplasm.[8] HBV enters cells via endocytosis and subsequently travels from early endosomes (EEs) to late endosomes (LEs)/lysosomes via RAB7, where uncoating of the virus occurs and HBV degradation is facilitated.[9] However, how HBV is trafficked from the cell surface to the nucleus has not been clarified fully.

Retrograde transport from endosomes to the trans-Golgi network (TGN) diverts proteins and lipids away from lysosomal degradation. Although several bacterial and viral proteins, including Shiga toxin (STX), cholera toxin, human papillomavirus 16, and human immunodeficiency virus-1 envelope protein, rely on retrograde transport to the TGN for correct delivery to target compartments,[10] the involvement of the Golgi apparatus in HBV infection has not been assessed.

Here, we reveal that DOCK11 regulated the GTPase-activating protein Arf-GAP with GTPase, ankyrin repeat, and pleckstrin homology domain-containing protein 2 (AGAP2), which plays important roles in the retrograde trafficking of cargo from EEs to the TGN, subsequently facilitating HBV retrograde transport from the EE-TGN-endoplasmic reticulum (ER) pathway to the nucleus for viral genome replication. A combinatorial treatment regimen incorporating entecavir (ETV) and DOCK11 ablation significantly restricted cccDNA levels *in vitro*. These observations suggest an unrecognized trafficking route of HBV from the cell surface to the nucleus via the TGN, which may facilitate the maintenance of cccDNA, and highlight DOCK11 as a potential therapeutic target for persistent HBV infection.

Results

DOCK11 Promotes HBV Replication in Hepatocytes

We identified human DOCK11 as a candidate host factor for the maintenance of persistent HBV infection in the HCC-derived HC1 cell line.[2] We established doxycycline (Dox)-induced DOCK11 overexpressing HepG2-NTCP-C4-Halo-DOCK11 cells, based on HepG2-NTCP-C4 cells.[11] HepG2-NTCP-C4-Halo-DOCK11 and control cells were infected with HBV virions from HepAD38 cells for 2 days. Dox treatment induced DOCK11 expression (Figure 1*A*), and DOCK11 overexpression increased HBV DNA and cccDNA levels compared with control cells (Figure 1*B–D*). Furthermore, we investigated the effects of DOCK11 on

***Authors share co-first authorship.**

Abbreviations used in this paper: **AGAP2, Arf-GAP with GTPase, ankyrin repeat, and pleckstrin homology domain-containing protein 2; ARF1, ADP ribosylation factor 1; BFA, brefeldin A; cccDNA, covalently closed circular viral DNA; CDC42, cell division cycle 42; CHB, chronic hepatitis B; COPI, coat protein I; DHR2, DOCK homology region 2; DOCK11, dedicator of cytokinesis 11; Dox, doxycycline; EE, early endosome; ER, endoplasmic reticulum; ETV, entecavir; GEF, guanine nucleotide exchange factor; GEq, genome equivalents; GFP, green fluorescent protein; HBcAg, HBV core antigen; HBcrAg, HBV core-related antigen; HBsAg, HBV surface antigen; HBV, hepatitis B virus; HCC, hepatocellular carcinoma; Ig, immunoglobulin; LE, late endosome; Luc, luciferase; NL, NanoLuc; NTCP, Na/taurocholate cotransporting polypeptide; PBS, phosphate-buffered saline; PCR, polymerase chain reaction; PXB cells, primary human hepatocytes; PLA, proximity ligation assay; RAB7KO, Rab7 knockout; RTD, real-time detection; shDOCK11, DOCK11 short hairpin RNA; shRNA, short hairpin RNA; siRNA, small interfering RNA; STX, Shiga toxin; TGN, trans-Golgi network.**

Most current article

2352-345X
https://doi.org/10.1016/j.jcmgh.2022.10.008

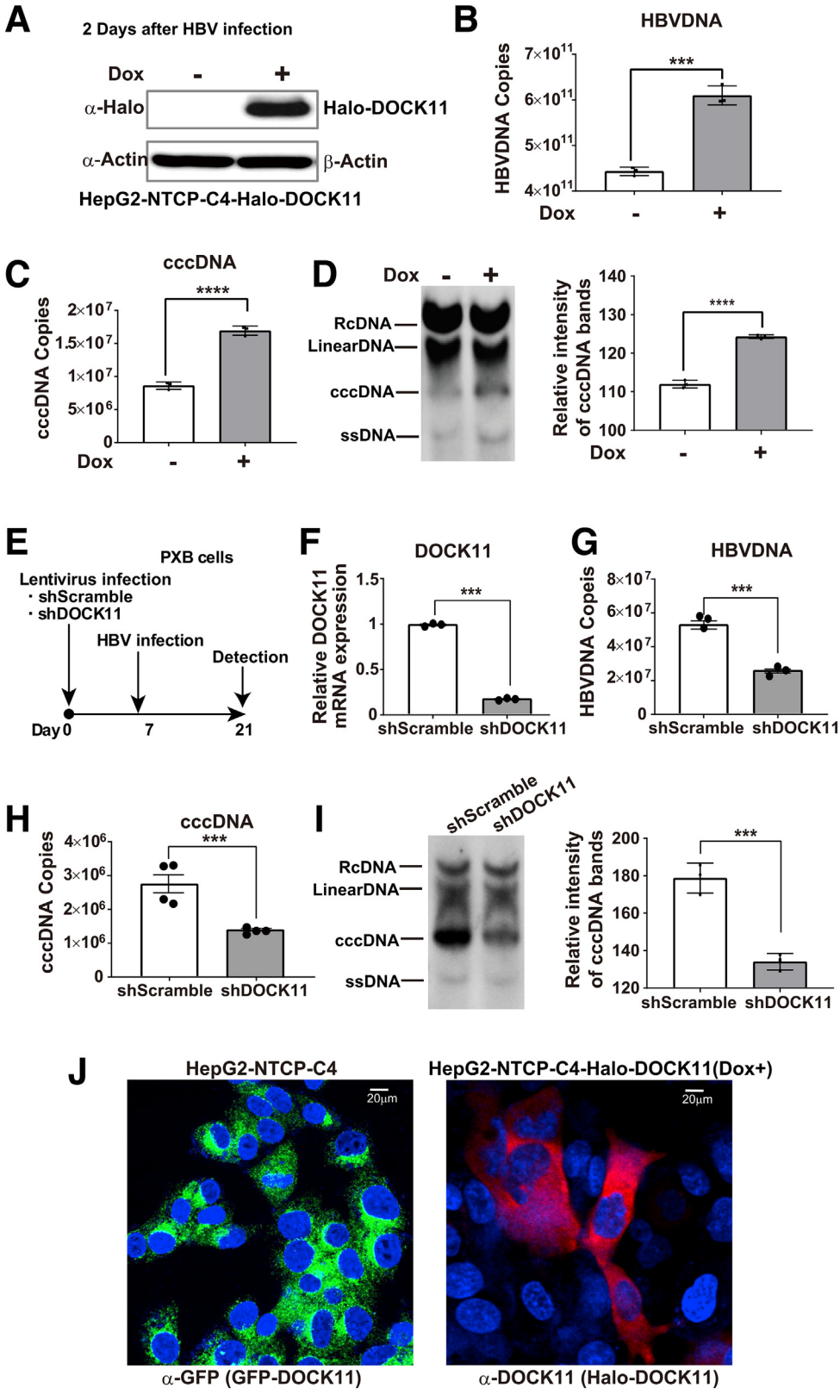

Figure 1. DOCK11 promotes HBV replication in hepatocytes. (*A–D*) Dox-treated HepG2-NTCP-C4-Halo-DOCK11 cells were infected with HBV particles from HepAD38 cells. DOCK11 induction was confirmed by immunoblotting (*A*), and HBV DNA and cccDNA levels were measured by RTD-PCR (*B* and *C*) and Southern blotting (D). (*E–I*) Effect of DOCK11 suppression on HBV replication in PXB cells. (*E*) Schedule of shDOCK11-lentivirus and HBV infection of PXB cells. shDOCK11-lentivirus transduction suppressed DOCK11 mRNA (*F*), HBV DNA (*G*), and cccDNA (*H* and *I*) levels in PXB cells as detected by RTD-PCR (*G* and *H*) and Southern blotting (*I*). (*J*) Intracellular localization of DOCK11 was examined using immunofluorescence analysis in HepG2-NTCP-C4 cells that were transiently transfected with GFP-DOCK11 and HepG2-NTCP-C4-Halo-DOCK11 cells in which DOCK11 expression was induced by Dox. Error bars, 20 μm. Representative results from 3 independent experiments are shown. $^{*}P < .05$, $^{**}P < .01$, $^{***}P < .001$, $^{****}P < .0001$.

HBV infection and replication using PXB cells (Figure 1*E*), which are fresh human hepatocytes taken directly from a PXB mouse liver (PhoenixBio Co, Ltd, Hiroshima, Japan). Ablation of DOCK11 expression in PXB cells by transduction with lentivirus expressing short hairpin RNA (shRNA) targeting DOCK11 (shDOCK11) (Figure 1*F*)

significantly suppressed HBV DNA and cccDNA levels (Figure 1*G–I*). Thus, DOCK11 promoted HBV replication in hepatocytes.

Immunofluorescence analysis showed that DOCK11 was predominantly localized in the cytoplasm of HepG2-NTCP-C4 cells transfected with GFP-DOCK11 and

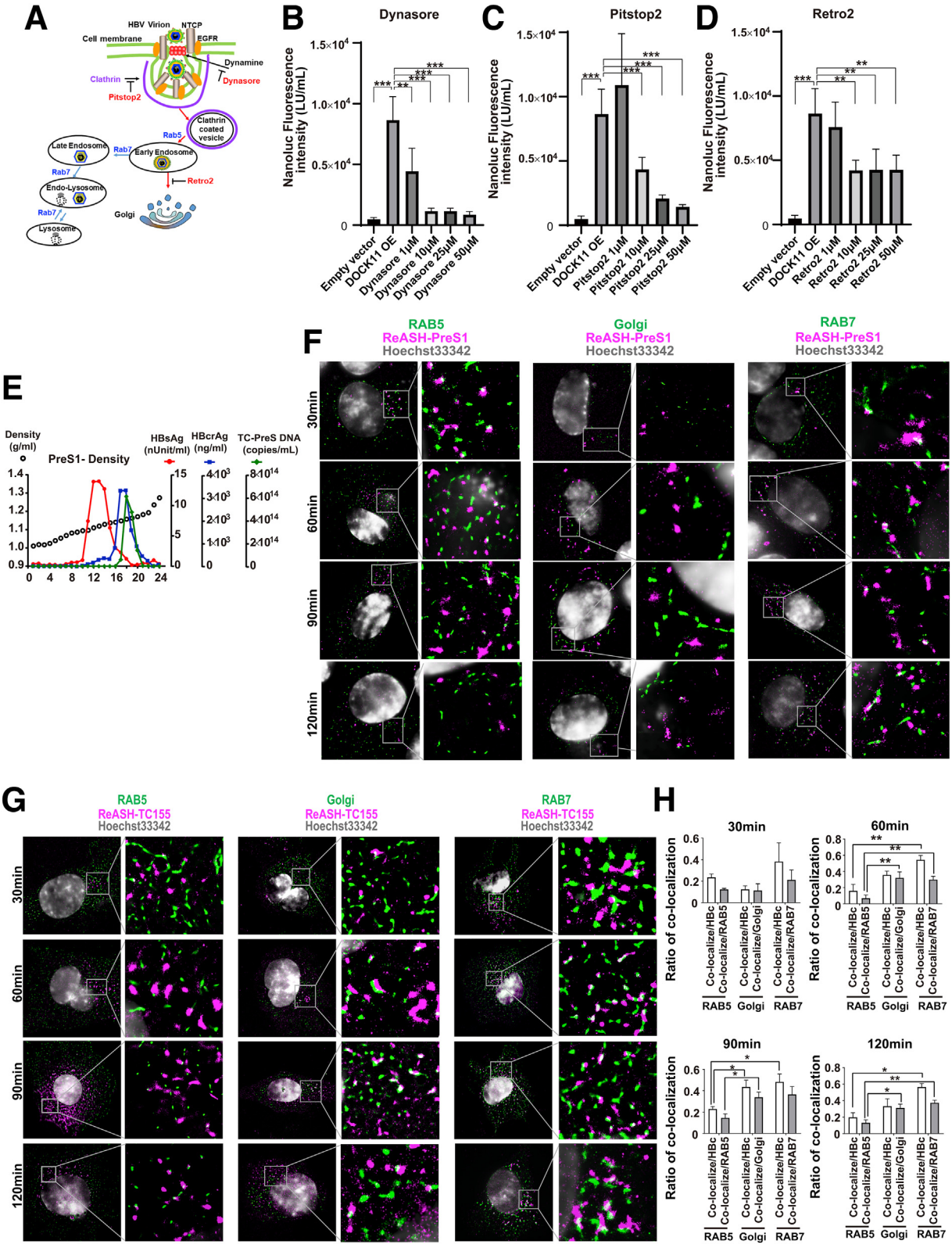

HepG2-NTCP-C4-Halo-DOCK11 stable cells in which DOCK11 was overexpressed by Dox treatment (Figure 1*J*).

HBV Uses an Alternative Retrograde Trafficking Route via the EE-TGN-ER Pathway

To examine which replication step was enhanced by DOCK11 overexpression, we used recombinant NanoLuc (NL)-HBV particles, which mimic the early stage of the HBV life cycle from entry to transcription/translation through cccDNA formation.[12] After transfection of HepG2-NTCP-C4 cells with the Halo-DOCK11 expression vector, we infected the cells with NL-HBV virions and measured luciferase (Luc) activity. DOCK11 overexpression substantially increased cccDNA-derived Luc activity by more than 5000-fold. The increased Luc activity was almost completely repressed by the entry inhibitors Dynasore (endocytosis inhibitor) and Pitstop 2 (clathrin inhibitor) (Figure 2*A*–*C*). These results indicated that DOCK11 enhanced the early stage of the HBV life cycle from entry to cccDNA formation. However, the step of the HBV life cycle affected by DOCK11 could not be determined because Dynasore and Pitstop 2 stopped HBV infection at the early entry stage. Interestingly, Retro-2, an inhibitor of cargo trafficking from EEs to the TGN (Figure 2*A*), significantly inhibited the DOCK11-induced enhancement of HBV infection (Figure 2*D*). After endocytosis, HBV enters EEs and then progresses to LEs-lysosomes via RAB7, where virus uncoating occurs, but the degradation of HBV is facilitated. We hypothesized that there is another trafficking pathway for HBV to reach the nucleus and initiate replication by escaping endosomal-lysosomal degradation (Figure 2*A*).

To visualize the trafficking route of HBV in cells, we constructed HBV particles in which capsid[15] or envelope proteins (newly developed in this study) were tagged with tetracysteine (C-C-P-G-C-C) and labeled with the ReAsH fluorescent dye. The locations of the fluorescent signals for HBV surface antigen (HBsAg) and HBV core antigen (HBcAg) were examined with green fluorescent protein (GFP)–labeled organelles. To distinguish subviral particles from infectious virions, we carried out iodixanol density gradient analysis. Appreciable titers of HBsAg, HBV core-related antigen (HBcrAg), and HBV DNA were found in fractions 17 and 18 (Figure 2*E*).

First, we confirmed that purified ReAsH-labeled HBV (ReAsH-TC155HBV and ReAsH-PreS1HBV) was infectious. At 30 minutes after infection with ReAsH-PreS1HBV, HBsAg was found within RAB5-positive structures (Figure 2*F*, Figure 3*A*). However, Myrcludex B treatment abolished the presence of HBsAg within RAB5-positive structures (Figure 3*A*). At 60 minutes after infection, HBcAg started to accumulate in the nucleus and increased at 90 and 120 minutes after infection (Figure 3*B*). Myrcludex B treatment abolished the nuclear accumulation of HBcAg (Figure 3*B*). We confirmed the synthesis of cccDNA by real-time detection (RTD)-polymerase chain reaction (PCR) (Figure 3*C* and *D*). Time-lapse images of live cells were captured after ReAsH-TC155HBV infection, and the accumulation of the HBcAg signal was clearly observed in the nucleus (Supplementary Videos 1–4). These results indicated that ReAsH-labeled HBV (ReAsH-TC155HBV and ReAsH-PreS1HBV) was infectious.

We then analyzed the detailed time course of ReAsH-labeled HBV (ReAsH-TC155HBV and ReAsH-PreS1HBV) by super-resolution fluorescence microscopy. At 30 minutes after infection, HBsAg was found within RAB5-positive structures, whereas HBcAg was barely detected (Figure 2*G*). At 60 minutes after infection, HBcAg was detected within the Golgi apparatus and RAB7-positive structures. The ratio of the detection of HBcAg (white) to the non-detection of HBcAg (red) in RAB5-positive (green), Golgi (green), and RAB7-positive (green) structures in different cells was calculated (Figure 2*H*). The ratio of HBcAg in Golgi and RAB7-positive structures (white) was significantly higher than that of RAB5-positive structures, except for before 30 minutes after infection (Figure 2*G* and *H*). The lower detection of HBcAg despite the presence of HBsAg in RAB5-positive structures (Figure 2*F*–*H*) might be because the fluorescent signal of HBcAg was masked by envelope proteins. Therefore, uncoating of the envelope proteins of HBV particles might take place after or during trafficking from EEs to LEs or the Golgi apparatus. These results clearly showed that there is an alternative trafficking route from EEs to the Golgi apparatus other than the classic trafficking route from EEs to LEs. Interestingly, HBsAg was found within RAB5-positive EEs and RAB7-positive LEs/lysosomes but not in the Golgi apparatus (Fig. 2*F*), suggesting that HBV particles may release capsids from EEs to the Golgi.

Next, to examine the functional relevance of RAB7 for HBV infection (Figure 4*A*), we established the HepG2-NTCP-C4-Rab7 knockout (RAB7KO) cell line, in which RAB7 was stably knocked out. Immunoblotting (Figure 4*B*) and immunofluorescence (Figure 4*C*) analysis confirmed that RAB7 was completely knocked out, but not other members

Figure 2. (***See previous page***). **Alternative retrograde trafficking route of HBV.** (*A*) Illustration of clathrin-mediated HBV entry into cells.[13,14] (*B–D*) HepG2-NTCP-C4 cells were transfected with the Halo-DOCK11 plasmid and then infected with NL-HBV particles. Luc activity derived from NL-HBV was measured. Cells were treated with Dynasore (*B*), Pitstop 2 (*C*), or Retro-2 (*D*). (*E*) TCPreS1-HBV was concentrated and applied to iodixanol density gradient analysis. After ultracentrifugation, 24 fractions were collected from the top of the gradient. The iodixanol density, HBsAg, HBcrAg, and HBV DNA levels were measured in each fraction. (*F*) HepG2-NTCP-C4 cells were infected with fractions 17 and 18. An HM-1000 super-resolution microscope was used to detect ReAsH-PreS1 (*red*) and RAB5, Golgi, and RAB7 (*green*). ReAsH-PreS1 within organelles showed *white signals*. (*G*) HepG2-NTCP-C4 cells were infected with fluorescently labeled ReAsH-TC155HBV. An HM-1000 super-resolution microscope was used to detect ReAsH-HBc (*red*) and RAB5, Golgi, and RAB7 (*green*). ReAsH-HBc within organelles showed *white signals*. (*H*) Ratio of the co-localization signals (*white*) in (*G*) versus HBV capsid (*red*) or organelles (*green*) was calculated. $^{*}P < .05$, $^{**}P < .01$.

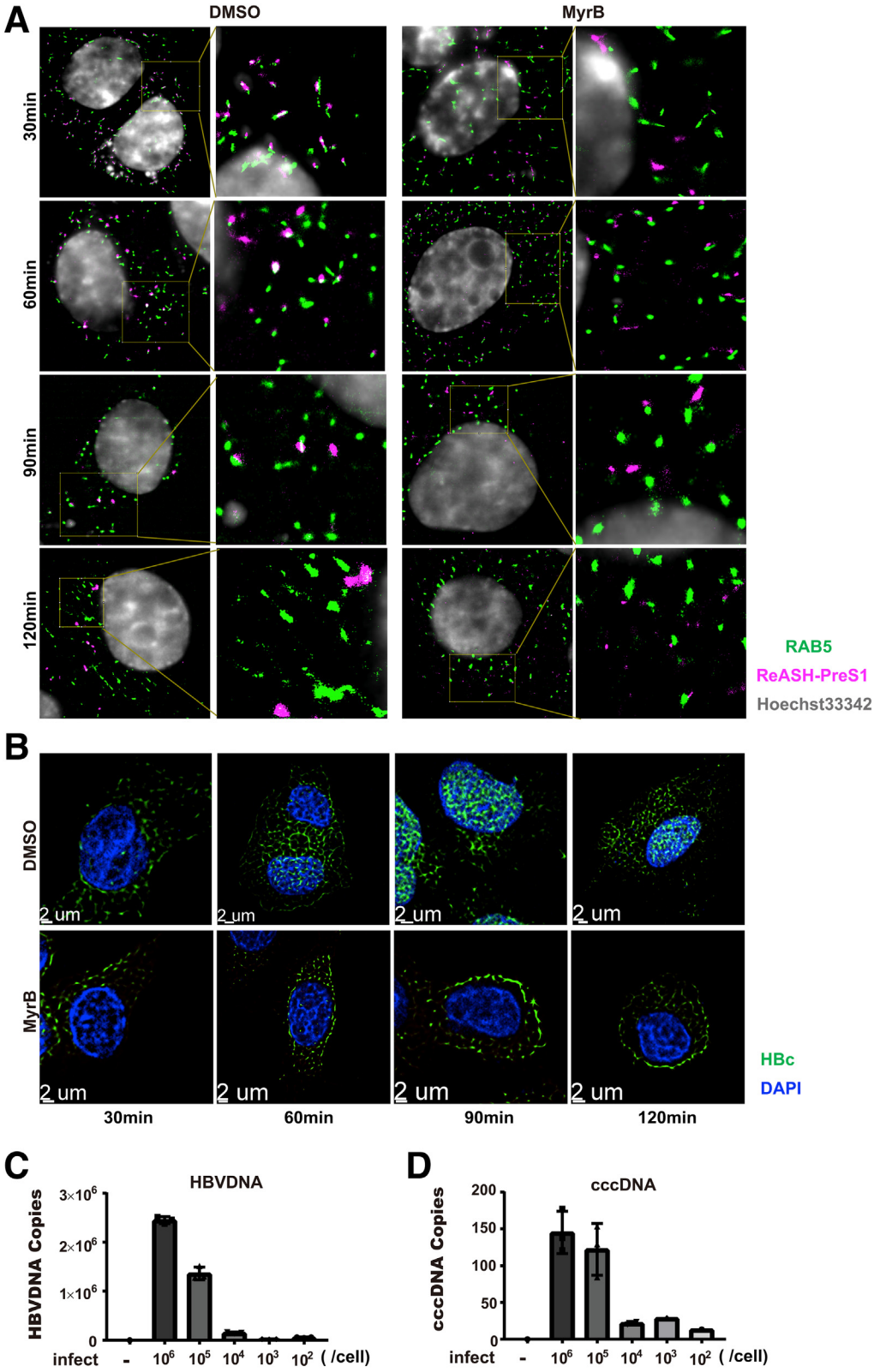

Figure 3. Functional analysis of HBV-TC-PreS1. TCPreS1-HBV was concentrated and applied to iodixanol density gradient analysis. HepG2-NTCP-C4 cells were infected with fractions 17 and 18, which were appreciable titers of HBsAg, HBcrAg, and HBV DNA, with or without 200 nmol/L Myrcludex B (MyrB) treatment. (*A*) An HM-1000 super resolution microscope was used to show the TCPreS1-HBV could enter into cells and found within RAB5-positive structure, whereas these could be blocked by MyrB. (*B*) Dragonfly confocal microscope of HBV capsid antigen (*green*) after TCPreS1-HBV infection with or without MyrB treatment at indicated time. Scale bars, 20 μm. (*C* and *D*) HBV DNA and cccDNA levels were detected by RTD-PCR after TCPreS1-HBV infection at indicated virions titers.

of the RAB family including RAB5, RAB9, and RAB11 (Figure 4*B*). Surprisingly, we observed that the loss of RAB7 rather increased the intracellular levels of HBV DNA and cccDNA after infection with HBV particles from HepAD38 cells (Figure 4*D*) or NL-HBV particles (Figure 4*E* and *F*). The increased intracellular levels of HBV DNA and cccDNA in RAB7KO cells were abrogated by Retro-2 treatment (Figure 4*E* and *F*). To examine the functional relevance of endo-lysosomes for HBV infection, we examined the effects of lysosome inhibitors on NL-HBV infection. Lysosome inhibitors did not decrease HBV infection but rather increased its replication (chloroquine) (Figure 4*G* and *H*).

To confirm the localization of incoming HBV in specific intracellular organelles by other methods, we performed a proximity ligation assay (PLA), an immune-based detection technique that generates a fluorescent signal only when 2 antigens of interest are within 40 nm of each other. After infection with NL-HBV particles, we tracked the HBV particles using an anti-HBcAg antibody and anti-RAB5 antibody (Figure 5*A*), TGN46 (a TGN marker, Figure 5*B*), or PDI (an ER marker, Figure 5*C*) in RAB7KO and control ScrambleKO cells. Clear punctate intracellular signals were generated after infection, which were significantly increased in RAB7KO cells compared with ScrambleKO cells (Figure 5*A*–*F*). Consistent with the PLA, immunofluorescence analysis by high-speed confocal microscopy and Pearson's and Manders' colocalization coefficients showed that NL-HBV particles were detected in RAB5-, TGN46-, and PDI-positive structures (Figure 5*G*–*I*). RAB7KO increased the localization of HBV in these organelles (Figure 5*J*–*L*). To further confirm these results, RAB7KO and ScrambleKO cells were infected with ReAsH-TC155HBV, and then time-lapse images of live cells were captured. Compared with the control cells, more HBV particles were transported to the TGN and ER in RAB7KO cells (Figure 6*A* and *B*, Supplementary Videos 1–4).

DOCK11 Promotes the Alternative Retrograde Trafficking Route of HBV via the EE-TGN-ER Pathway

To examine the roles of DOCK11 in the retrograde trafficking of HBV, DOCK11 expression was suppressed in RAB7KO cells and control ScrambleKO cells by DOCK11 small interfering RNA (siRNA) modified by GapmeR (Gene Design, Inc, Ibaraki, Japan). We observed that HBV DNA and cccDNA levels were repressed by DOCK11 suppression but not by ScrambleGapmeR treatment (Figure 7*A*–*C*). Immunofluorescence analysis showed that DOCK11 expression was detected within RAB5-, TGN46-, and PDI-positive structures (Figure 7*D*–*F*), and its expression was more obvious in DOCK11-overexpressing cells induced by Dox treatment (Figure 7*G*–*I*). Furthermore, in PXB cells, DOCK11 expression was also detected within TGN46- and GM130-positive (a marker of cis-Golgi) structures (Figure 7*J* and *K*). In addition, DOCK11 co-localized with HBcAg in Dox-treated HepG2-NTCP-C4-Halo-DOCK11 cells (Figure 7*L* and *M*) and PXB cells (Figure 7*N*). Immunoprecipitation analysis demonstrated the physical interaction of DOCK11 with HBV capsid at endogenous DOCK11 levels in HepG2-NTCP-C4 cells (Figure 7*O*) or at exogenous levels in Dox-treated HepG2-NTCP-C4-Halo-DOCK11 cells (Figure 7*P*) after infection with HBV virions derived from HepAD38 cells. These observations revealed that DOCK11 contributed to the retrograde trafficking of HBV via the EE-TGN-ER pathway in hepatoma cells and primary human hepatocytes.

AGAP2, a Member of the Arf-GAP Family, Is a Partner of DOCK11 and Contributes to the Retrograde Trafficking of HBV

To identify which proteins could interact with DOCK11 and might influence the retrograde trafficking of HBV via the EE-TGN-ER pathway, we performed liquid chromatography-tandem mass spectrometry metabolomics analysis on the Golgi fractions from Huh7-shDOCK11 cells, a DOCK11 stable knock-down cell line (Figure 8*A* and *B*), and identified the trafficking-associated protein AGAP2 as one of the down-regulated peptides.

We confirmed that knocking down DOCK11 mRNA reduced AGAP2 mRNA and protein levels (Figure 9*A*). Inducing DOCK11 expression increased AGAP2 mRNA and protein levels (Figure 9*B*). Furthermore, increasing DOCK11 levels increased AGAP2 protein expression in a dose-dependent fashion (Figure 9*C*). AGAP2 co-localized with DOCK11 in Dox-treated HepG2-NTCP-C4-Halo-DOCK11 cells (Figure 9*D*). In addition, immunoprecipitation of DOCK11 from HepG2-NTCP-C4 cells at endogenous protein level co-precipitated endogenous AGAP2 protein. In contrast, immunoprecipitation of AGAP2 from HepG2-NTCP-C4 cells co-precipitated DOCK11 (Figure 9*E*). Immunoprecipitation of exogenously expressed DOCK11 and AGAP2 in 293T cells that transfected with Halo-DOCK11 and Halo-AGAP2 was confirmed (Figure 9*F*).

We next explored the effects of AGAP2 on the intracellular levels of HBV DNA and cccDNA. Suppression of AGAP2 by siRNA significantly reduced HBV DNA and cccDNA levels in Dox-treated HepG2-NTCP-C4-Halo-DOCK11 cells (Figure 9*G*–*I*) and RAB7KO cells (Figure 9*J*–*L*). Furthermore, suppression of AGAP2 expression by shAGAP2-lentivirus transduction strongly reduced the intracellular levels of HBV DNA, cccDNA, and pregenomic RNA in PXB cells (Figure 9*M*–*P*). These results indicated that AGAP2 promoted HBV retrograde trafficking from EEs to the TGN, as reported previously for STX,[16] and AGAP2 depletion caused the retention of HBV in EEs. Thus, AGAP2 is a partner of DOCK11 and contributes to the retrograde trafficking of HBV.

DOCK11 and AGAP2 Regulate ADP Ribosylation Factor 1 Activity to Promote the Retrograde Trafficking of HBV

ADP ribosylation factor 1 (ARF1) was first reported to regulate intracellular vesicular trafficking from the Golgi apparatus to the ER and cycles between an active GTP-bound form and inactive GDP-bound form during cargo trafficking.[17] DOCK11 is a GEF protein that contributes to cellular signaling by activating small G proteins, and AGAP2

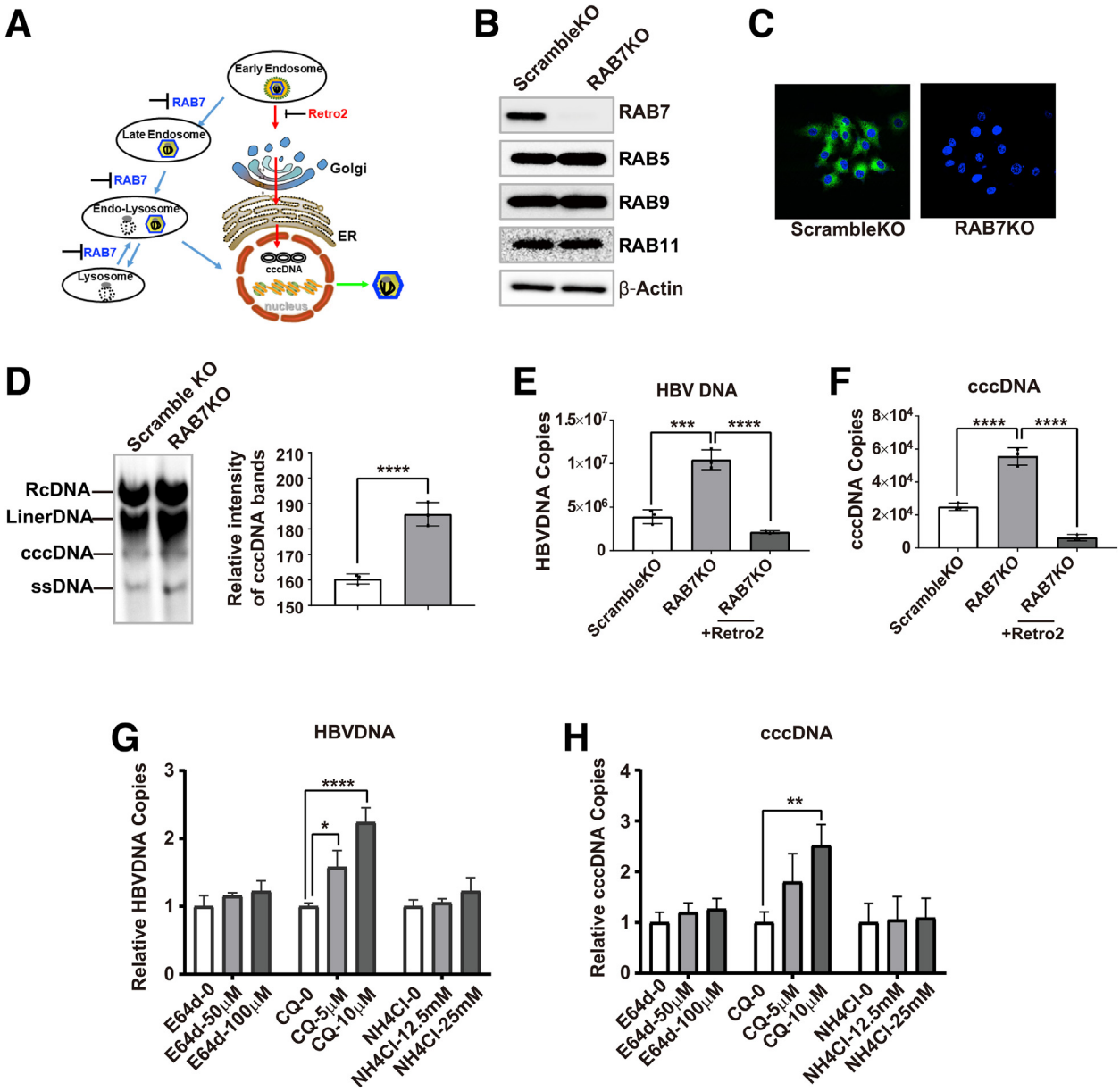

Figure 4. Retrograde trafficking route of HBV can be increased by RAB7KO or a lysosome inhibitor. (*A*) Illustration of the functional relevance of RAB7 for HBV infection. (*B*) Immunoblotting analysis of RAB7 and other RAB proteins (RAB5, RAB9, and RAB11) in HepG2-NTCP-C4-RAB7KO or control cells. (*C*) Immunofluorescence analysis of RAB7 protein in RAB7KO or control cells. (*D–F*) RAB7KO or control cells were infected with HBV particles from HepAD38 cells (*D*) or NL-HBV particles (*E* and *F*) with or without Retro-2 treatment for 30 hours. HBV DNA and cccDNA levels were detected by Southern blotting (*D*) or RTD-PCR (*E* and *F*). (*G* and *H*) HepG2-NTCP-C4 cells were infected with NL-HBV particles for 30 hours and treated with lysosome inhibitors including E46d, chloroquine (CQ), and NH_4Cl. Genomic DNA was extracted, and the levels of HBV DNA and cccDNA were measured by RTD-PCR. Representative results from 3 independent experiments are shown. $^{*}P < .05$, $^{**}P < .01$, $^{***}P < .001$, $^{****}P < .0001$.

has high GAP activity toward ARF1.[18] Therefore, we hypothesized that DOCK11 would have GEF activity toward ARF1 and that AGAP2 would have GAP activity toward ARF1. Immunoprecipitation of DOCK11 or AGAP2 co-precipitated ARF1 at endogenous and exogenous levels (Figure 10*A* and *B*). Moreover, immunoprecipitation of ARF1 co-precipitated DOCK11 and AGAP2 (Figure 10*A* and *B*). Thus, ARF1 formed a complex with DOCK11 and AGAP2.

We next assayed GEF or GAP activity using recombinant DOCK11-DHR2 domain, AGAP2, CDC42, and ARF1 proteins *in vitro*. The GEF activity of DOCK11 for CDC42 is reported to originate from its DHR2 domain.[6] We confirmed that the DOCK11-DHR2 domain was sufficient to promote HBV infection (Figure 10*C–E*). We also confirmed that DOCK11 exhibited GEF activity toward CDC42 (Figure 10*F*), as reported previously. We further found that DOCK11 exhibited

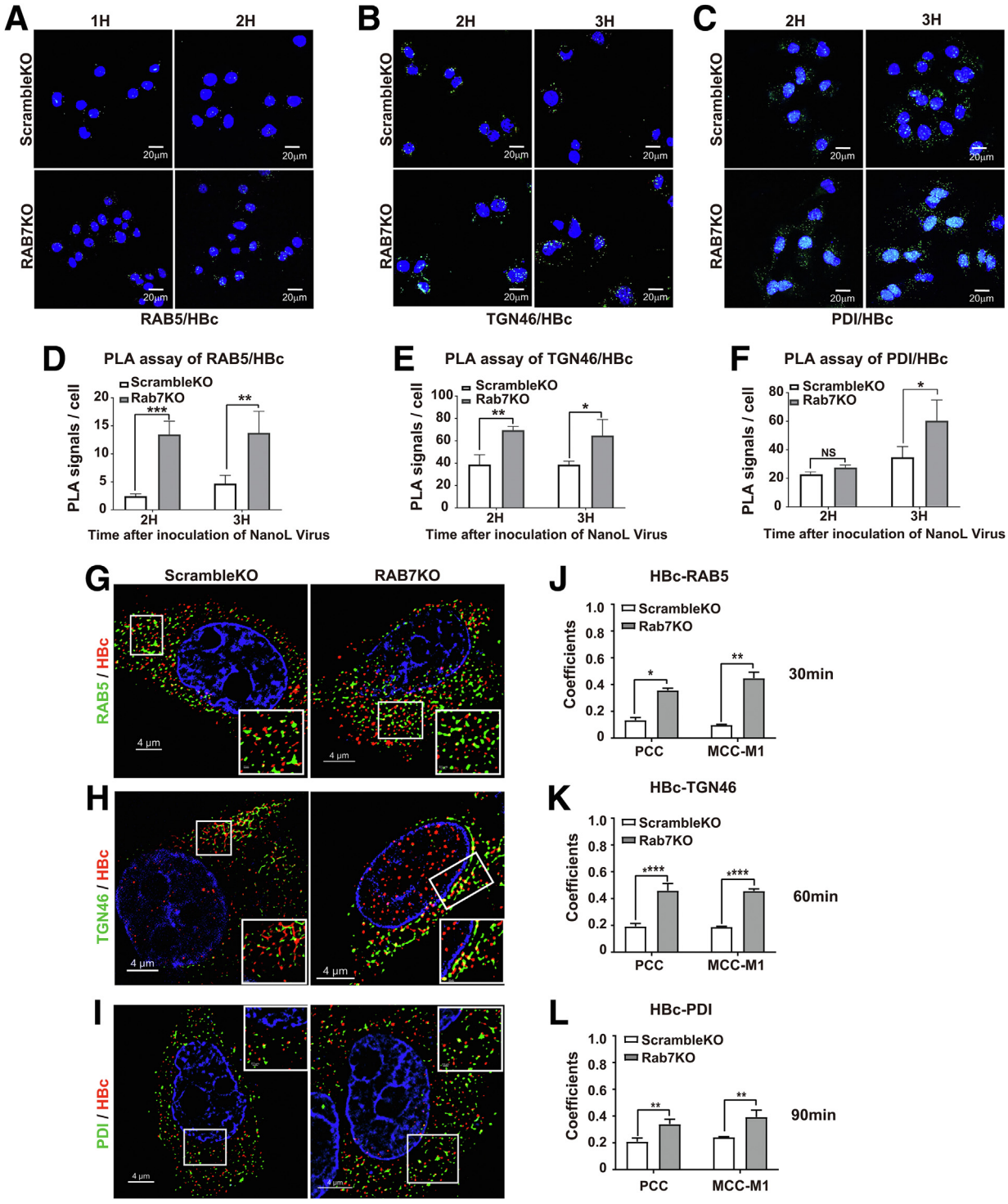

Figure 5. HBV is found in the organelles of retrograde EE-TGN-ER trafficking route. (*A–C*) RAB7KO or control cells were infected with NL-HBV particles. After 1 to 3 hours, PLA was performed, and images were captured by confocal microscopy. Fluorescence micro-signals of the PLA indicated the HBV capsid might be localized in RAB5- (*A*), TGN46- (*B*), and PDI-positive (*C*) organelles. Scale bars, 20 μm. (*D–F*) PLA fluorescence intensity per cell in each sample of *A–C* was processed by ImageJ software. (*G–I*) Dragonfly confocal microscopy of HBV capsid antigen (*red*) and RAB5, TGN46, and PDI (*green*) in RAB7KO or control cells at 30 minutes (*G*), 60 minutes (*H*), and 90 minutes (*I*) after infection with NL-HBV particles. *Yellow signals* indicating HBV capsids (*red*) were found in those organelles (*green*). (*J–L*) Changes of Pearson's correlation coefficient (PCC) and Manders' correlation coefficient (MCC-M1) in panels *G–I*. Scale bars, 4 μm. Representative results from 3 independent experiments are shown. $^{*}P < .05$, $^{**}P < .01$, $^{***}P < .001$, $^{****}P < .0001$.

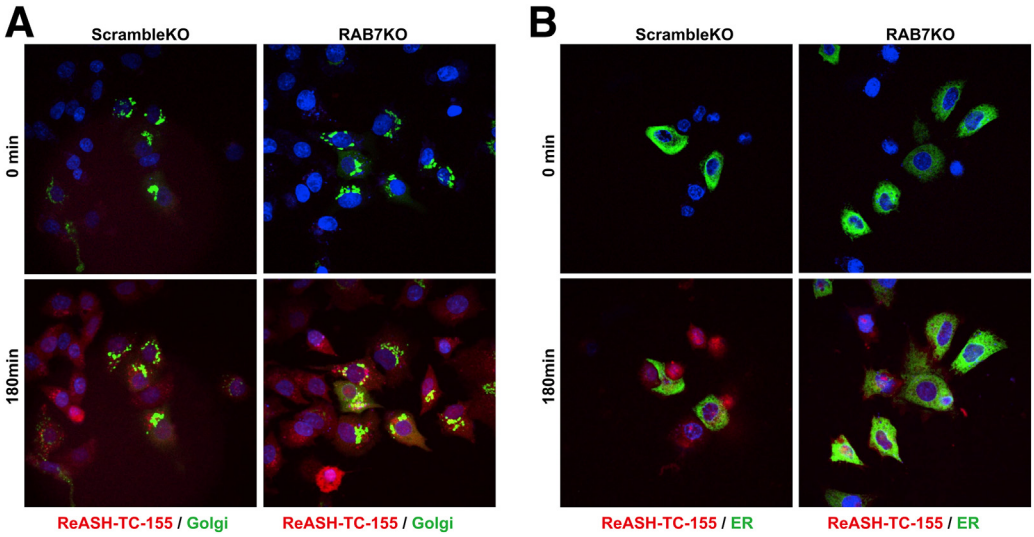

Figure 6. Time-lapse analysis of fluorescently labeled HBV infection. HepG2-NTCP-C4-RAB7KO and control cells were seeded in a chamber slide and incubated with CellLight Golgi-GFP or ER-GFP for the labeling of each organelle. Next day, the medium was replaced with fresh growth medium containing Hoechst 33342 for another 30 minutes. Then, the cells were infected with ReASH-TC155HBV virions, and time-lapse analysis was applied. *Reds* are HBV capsids, and greens are Golgis or ERs. Time-lapse images showed more retrograde transport of HBV capsid to the Golgi (*A*) and ER (*B*) in HepG2-NTCP-C4-RAB7KO cells compared with control cells (Supplementary Videos 1–4).

GEF activity and that AGAP2 had GAP activity toward ARF1 (Figure 10*G* and *H*). Brefeldin A (BFA) is an inhibitor of ARF1 activation by preventing GDP/GTP exchange. Treatment of RAB7KO cells with BFA abrogated the increased intracellular levels of HBV DNA and cccDNA (Figure 10*I* and *J*). Moreover, the concentration of HBcAg in the Golgi fraction was increased in RAB7KO cells but was reduced by BFA treatment (Figure 10*K*). Furthermore, NAV-2729, another ARF1 inhibitor, also abrogated the intracellular levels of HBV DNA and cccDNA in RAB7KO cells (Figure 10*L* and *M*). Binding of DOCK11 and AGAP2 might be beneficial for recruiting ARF1 to DOCK11 and AGAP2, and GTP-bound ARF1 and GDP-bound ARF1 were both required for efficient trafficking (Figure 10*N*). In addition, retrograde trafficking of STX from EEs to the TGN and subsequently to the ER could be blocked by 2 μmol/L BFA (Figure 11*A*). Similarly, retrograde trafficking of HBcAg could also be blocked by the same concentration of BFA (Figure 11*B*).

Intracellular transport is mediated by transport vesicles that are often coated with coat proteins. Coat protein I (COPI)-coated vesicles mediate transport between Golgi stacks or from the Golgi to the ER. We next determined whether suppressing COPI in RAB7KO cells affected NL-HBV retrograde transport to the nucleus through the TGN and ER. COPI siRNA treatment of RAB7KO cells decreased HBV DNA and cccDNA levels (Figure 12*A*–*C*). A PLA further revealed that treatment of RAB7KO cells with COPI siRNA decreased the punctate fluorescent signals generated by PDI and HBcAg (Figure 12*D* and *E*), whereas the punctate fluorescent signals generated by TGN46 and HBcAg were increased (Figure 12*F* and *G*), indicating that COPI depletion prevented NL-HBV capsid trafficking via the TGN-ER route and induced NL-HBV capsid stacking in the TGN.

DOCK11 Expression Is Associated With Entecavir Treatment in Vivo and in Vitro

To investigate the role of DOCK11 in patients with CHB, we examined DOCK11 gene expression in biopsied liver samples from 17 patients with CHB before and after ETV treatment. The patients were administered ETV because of the elevation of HBV DNA in serum. Compared with before ETV treatment, DOCK11 expression was significantly reduced after ETV treatment in CHB patients (Figure 13*A*). Consistently, serum HBsAg and HBV DNA levels were significantly reduced by ETV treatment, although the reduction of HBsAg was not obvious compared with the reduction of HBV DNA (Figure 13*B* and *C*). Because HBsAg serum levels have been reported to be well-correlated with cccDNA levels in the liver, Spearman's correlation analysis between the reduction of HBsAg and DOCK11 levels showed that the reduction of HBsAg was significantly correlated with that of DOCK11 (Figure 13*D*), suggesting important roles for DOCK11 in the maintenance of cccDNA in the liver of patients with CHB.

To examine the effect of the combination of ETV treatment and the suppression of DOCK11 expression, we used HepG2 cells derived from HepAD38 cells in which HBV expression was regulated by the CMV-tet promoter *in vitro*. The shDOCK11-lentivirus transduction of HepAD38 cells (HepAD38-shDOCK11) (Figure 13*E*) suppressed HBV DNA and cccDNA formation according to Southern blotting and RTD-PCR (Figure 13*F*–*I*). The suppression of cccDNA by shDOCK11 was more obvious (78% reduction) (Figure 13*I*, left) than for ETV treatment (65% reduction) (Figure 13*I*, right). Interestingly, the combination of ETV plus shDOCK11 further reduced HBV DNA and cccDNA levels by 95% and 85%, respectively, compared with ETV alone treatment by 88% and 65% (Figure13*H*, right

and *I*, right). Similar results were obtained using HepG2.2.15 cells in which HBV transcription is mediated by its own promoter (Figure 13*J–L*). Interestingly, consistent with our biopsied liver samples, DOCK11 expression was significantly reduced after ETV treatment compared with before ETV treatment in these cell lines (Figure 13*E* and *J*).

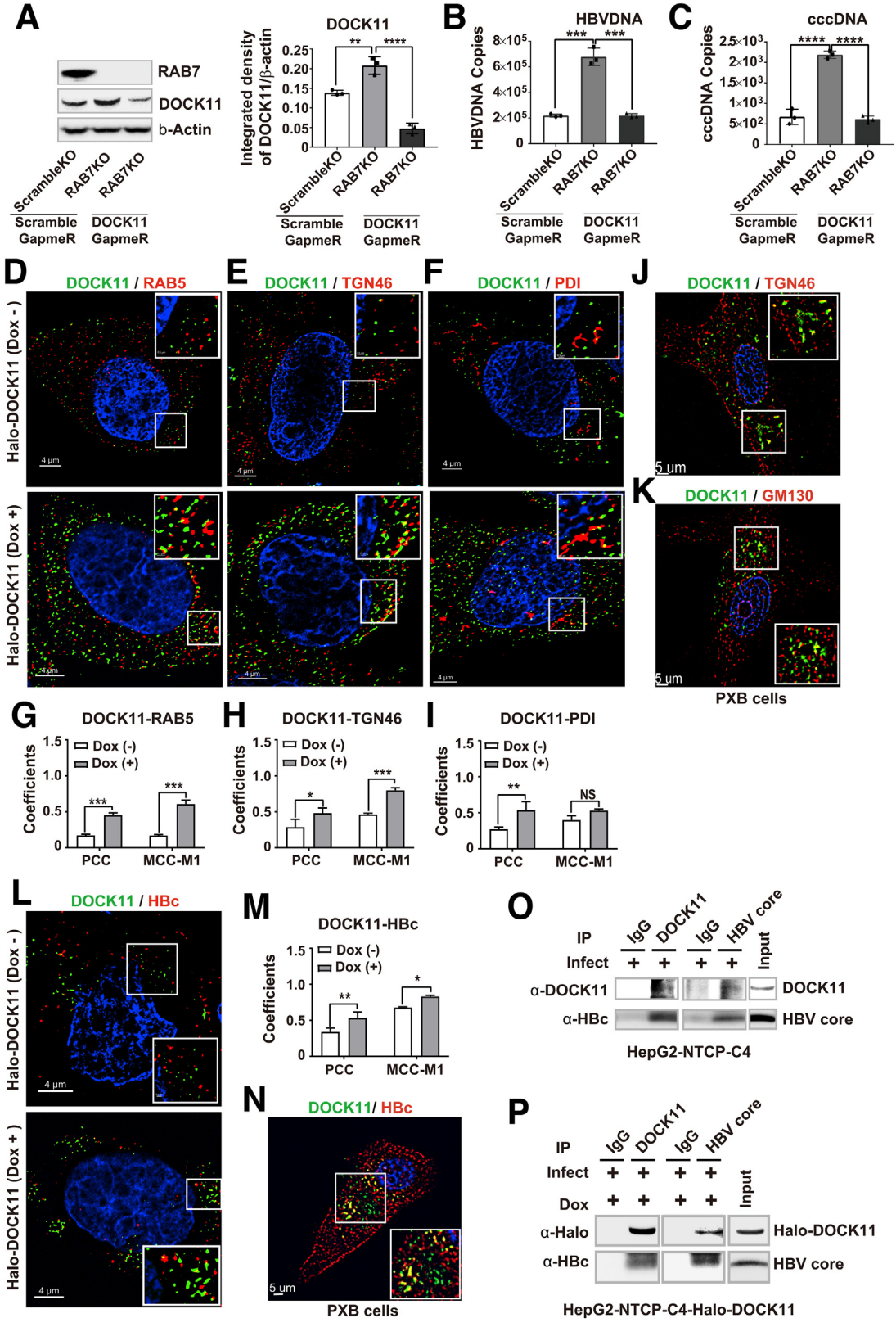

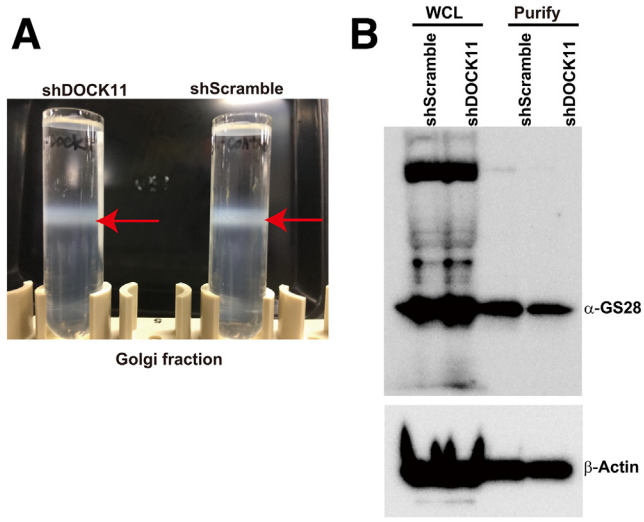

Figure 8. Extraction of the Golgi fraction from hepatocytes for proteome analysis. (*A*) The Golgi fraction was extracted from DOCK11-depleted Huh7-shDOCK11 cells and control Huh7-shScramble cells. (*B*) Verification of the Golgi fraction by immunoblotting using an anti-GS28 antibody.

Discussion

In this study, we found that HBV used a unique retrograde trafficking route via the EE-TGN-ER pathway to the cell nucleus that had not been implicated previously in HBV infection. This trafficking route could be beneficial for HBV by avoiding lysosomal degradation and thereby facilitating the maintenance of cccDNA in the nucleus. Interestingly, we showed that DOCK11 accelerated this pathway.

DOCK11 is a member of the Zizimin/DOCK family of GEFs and is a prominent GEF for CDC42.[6] Moreover, the activation of CDC42 together with its downstream target WASP and the γCOP subunit of the COPI complex influences F-actin organization and Golgi apparatus integrity and regulates Golgi-to-ER transport.[19,20] However, a recent report showed that CDC42 appears to promote intra-Golgi anterograde transport rather than affecting COPI transport back to the ER.[21] Therefore, it is unlikely that CDC42 is involved directly in the retrograde nuclear trafficking of HBV via the EE-TGN-ER pathway identified in this study.

To clarify the direct mechanism by which DOCK11 participates in the retrograde trafficking of HBV, we identified AGAP2 as a novel partner of DOCK11 using liquid chromatography-tandem mass spectrometry. AGAP2 is a crucial regulator of retrograde transport together with ARF1, a representative GTP-binding protein involved in retrograde protein trafficking of STX, cholera toxin, and the endogenous proteins TGN46 and mannose 6-phosphate receptor.[16] ARF1 changes between active GTP-bound and inactive GDP-bound conformations, depending on GEFs for activation and GTPase-activating proteins for inactivation.[19] Notably, we showed that DOCK11 and AGAP2 formed a complex and could bind to ARF1, DOCK11 exhibited GEF activity, and AGAP2 had GAP activity toward ARF1 (Figures 9 and 10). It was interesting that DOCK11 induced AGAP2 expression, and they formed a complex, which might be beneficial for recruiting ARF1 to this complex. ARF1 was activated by DOCK11 and deactivated by AGAP2 continuously, which would facilitate the efficient recycling of vesicles and cargo release during HBV retrograde trafficking (Figure 10). Moreover, we showed that DOCK11 could bind to HBcAg, which is also advantageous for DOCK11 to facilitate the recruitment of HBV capsids to retrograde trafficking (Figure 7). ARF1 regulates COPI vesicles that mediate transport between Golgi stacks or from the Golgi to the ER.[22] We also showed that the depletion of COPI could prevent NL-HBV capsid transport into the nucleus of RAB7KO cells (Figure 12), indicating the involvement of the trafficking route from the TGN to ER for HBV infection.

Previous reports showed that HBV enters cells via endocytosis and subsequently travels from EEs to lysosomes via RAB7, where uncoating of the virus occurs and HBV degradation is facilitated.[9] In this study, we showed that RAB7A was not necessary for HBV infection but rather decreased HBV infection (Figure 4). RAB7KO cells were more suspectable to HBV infection, as shown by the increased intracellular levels of HBV DNA and cccDNA after infection with HBV particles from HepAD38 cells (Figure 4*D*) or NL-HBV particles (Figure 4*E* and *F*). This finding was also supported by the increased PLA fluorescent punctate intracellular signals in RAB7KO cells (Figure 5). Thus, we showed that the retrograde trafficking route through the EE-TGN-ER pathway to the nucleus could be more efficient than that previously recognized through the EE-LE pathway to the nucleus.

Figure 7. (***See previous page***). **DOCK11 facilitates the retrograde trafficking of HBV via the EE-TGN-ER pathway.** (*A–C*) HepG2-NTCP-C4-RAB7KO and control cells were transiently transfected with DOCK11 siRNA modified by GapmeR, and then the cells were infected with recombinant NL-HBV particles for 30 hours. DOCK11 protein and mRNA (*A*), HBV DNA (*B*), and cccDNA (*C*) levels were detected by immunoblotting and RTD-PCR. (*D–I*) Dragonfly confocal microscopy of HepG2-NTCP-C4-Halo-DOCK11 cells with or without Dox treatment. Dox-induced DOCK11 expression was found within the RAB5- (*D*), TGN46- (*E*), and PDI-positive (*F*) organelles. The positive signals of DOCK11 in the above organelles were comparable in the cells with or without Dox treatment. (*J* and *K*) Dragonfly confocal microscopy of PXB cells. Endogenous DOCK11 was present in the TGN46- (*J*) and GM130-positive (*K*) organelles. (*L*) Dox-treated or non-treated HepG2-NTCP-C4-Halo-DOCK11 cells were infected with NL-HBV particles for 2 hours, and the co-localization of DOCK11 and HBcAg was analyzed under a Dragonfly confocal microscope. (*M*) Changes of Pearson's correlation coefficient (PCC) and Manders' correlation coefficient (MCC-M1) in panel *L*. (*N*) Co-localization of endogenous DOCK11 and HBV capsid antigen in PXB cells. (*O* and *P*) Co-immunoprecipitation of DOCK11 and HBcAg in HepG2-NTCP-C4 cells (Endogenous) (*O*) or HepG2-NTCP-C4-Halo-DOCK11 cells with Dox treatment (Exogenous) (*P*). Cells were infected with HBV particles from HepAD38 cells for 3 hours. Representative results from 3 independent experiments are shown. $^{*}P < .05$, $^{**}P < .01$, $^{***}P < .001$, $^{****}P < .0001$.

For many viruses, acidification-mediated proteinase activation in lysosomes is helpful for uncoating and the establishment of infection. However, HBV infection is pH-independent[23] and possibly mediated by translocation motifs,[24] which may preserve viral morphology. In this study, lysosome inhibitors did not reduce HBV infection, which was

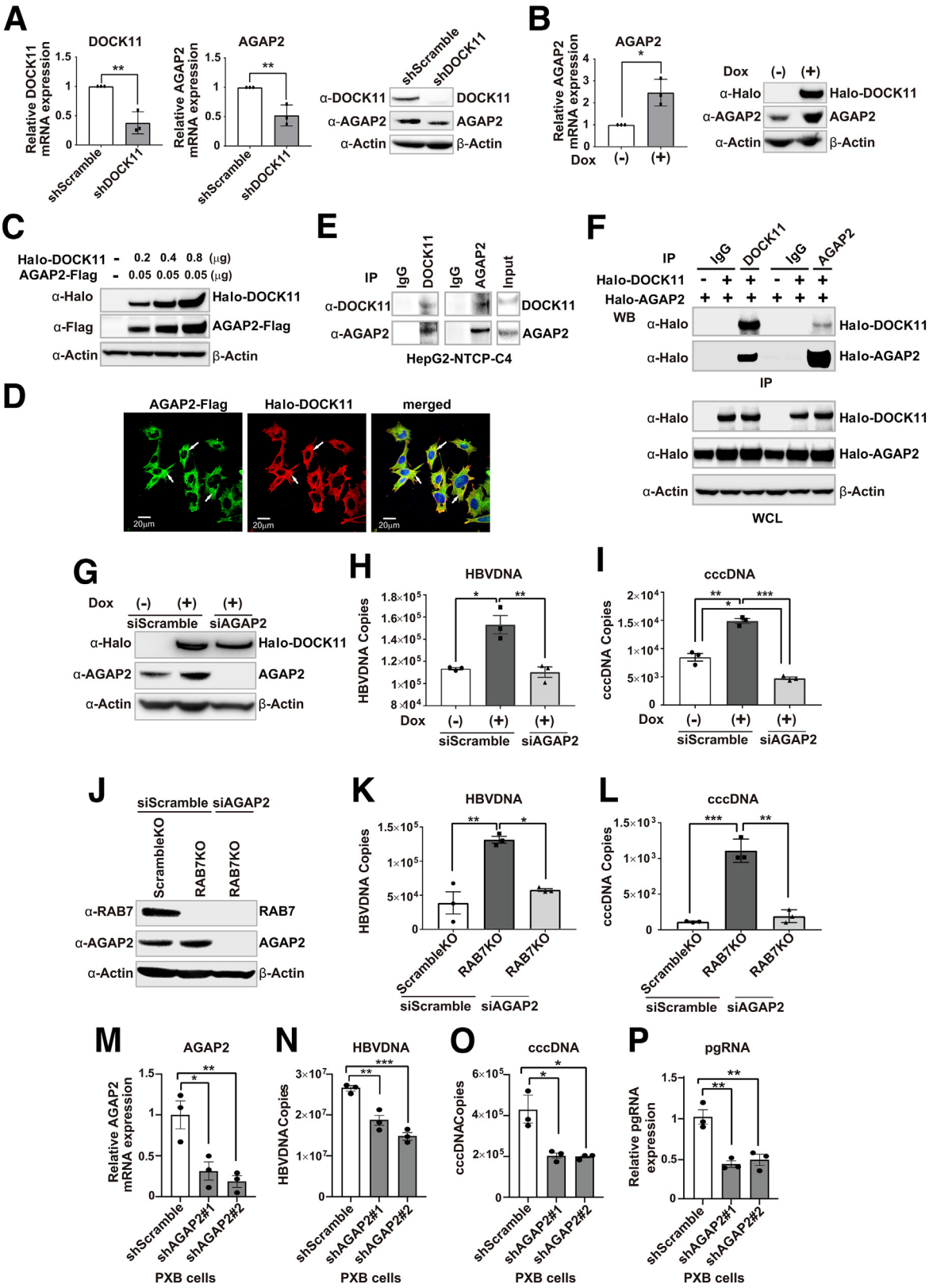

compatible with previous findings.[23,25] Therefore, conformational changes of the viral envelope rather than its extensive degradation might be sufficient for HBV uncoating.

Super-resolution microscopy of fluorescently labeled capsid and surface antigens of infected HBV particles suggested that the uncoating of envelope protein might occur at a relatively early phase after or during trafficking from EEs to LEs or EEs to the TGN (Figure 2). Interestingly, in duck HBV, TGN host proteins such as carboxypeptidase D[26] and furin[27] participate in viral entry and cleavage of the large envelope protein for infection. Therefore, in HBV, Golgi host proteins might be involved in infection, and thus, retrograde trafficking of HBV from EEs to the TGN is not peculiar.

What is the role of retrograde trafficking from the EE-TGN-ER pathway to the nucleus in the pathogenesis of HBV infection? This trafficking route separates cargo from the cytosol by a membrane, which could protect HBV from cytosolic innate immune responses that mediate viral degradation. Moreover, naked viral capsids could be the target of protein degradation pathways such as ubiquitination-proteasome and autophagy. It could be speculated that during active replication, a large amount of virus would go to the classic lysosomal pathway, and the virus that "spills over" from lysosomal degradation continues to replicate. During inactive replication, a small amount of virus would use the retrograde pathway through the Golgi, thereby avoiding lysosomal degradation and maintaining replication. Further study is necessary to reveal the regulation of these 2 pathways.

In the liver of CHB patients, we showed that ETV treatment significantly decreased DOCK11 expression together with decreased HBV replication (Figure 13*A*–*C*). The decreased expression of DOCK11 might be reflected in the reduced replication of HBV in hepatocytes, because we found that DOCK11 levels are increased in primary human hepatocytes by HBV infection. Furthermore, the reduction of HBsAg was significantly correlated with that of DOCK11 (Figure 13*D*), indicating that cccDNA could be regulated by DOCK11 in the liver of CHB patients. In addition, the combination of knocking down DOCK11 together with ETV treatment further suppressed HBV replication compared with either factor alone. These findings highlighted the substantial potential for developing therapeutics that target DOCK11 in CHB patients. The possible involvement of DOCK11 in HBV replication should be explored further.

Although our study showed that DOCK11 activated the retrograde trafficking of HBV from the EE-TGN-ER pathway to the cell nucleus, it is not known how the nucleocapsid released from the ER enters the nucleus. Although the intrinsic mechanisms are not yet known, there are connections between the ER and nuclear membrane, and a recent report showed that lipid droplets generated in the ER lumen can move into the nucleoplasm of hepatocytes by a precise molecular mechanism.[28] It was also reported that HBV capsid combined with lipid droplets could efficiently establish infection.[29] Therefore, ER stress-induced lipid droplets in the ER potentially participate in the retrograde trafficking of HBV via the EE-TGN-ER pathway to the cell nucleus.

DOCK11 may also potentially increase HBV infection by increasing the uptake of HBV at the entry level because endocytosis is mediated by actin polymerization on the cell surface, and this process is regulated by CDC42. Moreover, further studies should be performed to uncover the roles of DOCK11 in cccDNA formation in the nucleus because confocal microscopy revealed the low-level expression of DOCK11 in the nucleus.[30]

In conclusion, our findings might lead to the identification of new areas in the early steps of the HBV life cycle as well as facilitate the development of molecular targeting therapies to cure HBV infection.

Materials and Methods

Key resources are shown in Table 1, and the oligonucleotides for shRNA, CRISPR/Cas9, cloning, and RTD-PCR are shown in Table 2.

Patients

DOCK11 expression was evaluated using non-tumor liver biopsied specimens from 17 HBV-infected HCC patients before and after ETV therapy. HBsAg and HBV DNA levels were evaluated in serum samples isolated by centrifugation of coagulated whole blood and preserved at −80°C. The research protocols were reviewed by the ethics committee at Kanazawa University and its related hospitals. Informed consent was obtained from all patients.

Figure 9. (***See previous page***). **AGAP2 is a partner of DOCK11 and contributes to the retrograde trafficking of HBV.** (*A*) Endogenous DOCK11 and AGAP2 mRNA and protein in Huh7-shDOCK11 or Huh7-shScramble cells were analyzed by RTD-PCR and immunoblotting. (*B*) Inducible expression of DOCK11 by Dox treatment increased the expression of AGAP2 mRNA and protein. (*C*) Transient overexpression of DOCK11 increased AGAP2 protein levels in dose-dependent manner in 293T cells. (*D*) DOCK11 co-localized with AGAP2 protein in Dox-treated HepG2-NTCP-C4-Halo-DOCK11 cells that were transfected with the AGAP2-Flag plasmid. Scale bars, 20 μm. (*E* and *F*) Co-immunoprecipitation of DOCK11 and AGAP2 in HepG2-NTCP-C4 cells (Endogenous) (*E*) or in 293T cells that were co-transfected with the Halo-DOCK11 and Halo-AGAP2 plasmid (Exogenous) (*F*). (*G*–*I*) Dox-treated HepG2-NTCP-C4-Halo-DOCK11 cells were transfected with AGAP2 siRNA or Scramble siRNA, and the cells were then infected with NL-HBV particles for 30 hours. Halo-DOCK11 and endogenous AGAP2 protein (*G*), HBV DNA (*H*), and cccDNA (*I*) levels were detected by immunoblotting and RTD-PCR. (*J*–*L*) HepG2-NTCP-C4-RAB7KO cells were transfected with AGAP2 siRNA or Scramble siRNA, and the cells were then infected with NL-HBV particles for 30 hours. AGAP2 protein (*J*), HBV DNA (*K*), and cccDNA (*L*) levels were detected by immunoblotting and RTD-PCR. (*M*–*P*) PXB cells were infected with the shAGAP2-lentivirus or shScramble-lentivirus and then infected with HBV virions (PhoenixBio). AGAP2 mRNA (*M*), HBV DNA (*N*), cccDNA (*O*), and pregenomic RNA (pgRNA) (*P*) levels were detected by RTD-PCR. Representative results from 3 independent experiments are shown. $^{*}P < .05$, $^{**}P < .01$, $^{***}P < .001$, $^{****}P < .0001$.

Cell Lines

The human liver cancer Huh7, HepG2-NTCP-C4, HepG2.2.15, and HepAD38 cell lines were authenticated by DNA fingerprinting in 2016. Primary human hepatocytes (PXB cells) and their specific medium were purchased from PhoenixBio Co, Ltd (Hiroshima, Japan). The Huh7 and

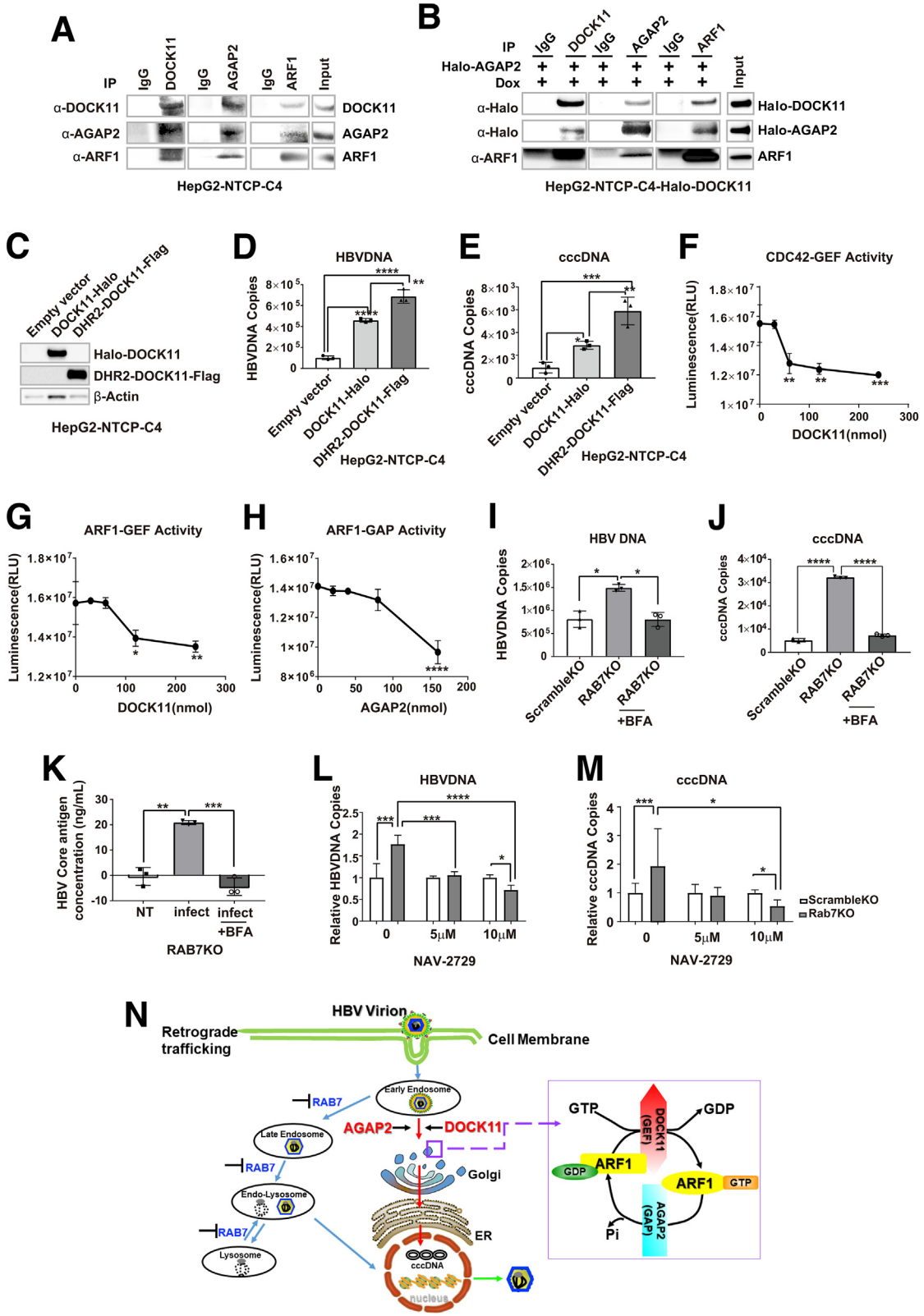

HepG2.2.15 cell lines were maintained in Dulbecco modified Eagle medium (Life Technologies, Carlsbad, CA), and the other cell lines we established were cultured in Dulbecco modified Eagle medium/F-12, GlutaMAX supplement (Thermo Fisher Scientific, Waltham, MA); both media contained 10% fetal bovine serum, 100 U/mL penicillin, and 100 μg/mL streptomycin. The addition of 400 μg/mL G418, 10 mmol/L HEPES buffer solution, and 5 μg/mL insulin was needed for the culture of the HepG2-NTCP-C4 and HepAD38 cell lines.

HBV Preparation

HepAD38 cell culture supernatant filtered through 0.45-μm VWR filter units was mixed with PEG 8000 (40% wt/vol; Sigma-Aldrich, St Louis, MO) containing 800 mmol/L NaCl to a final concentration of 10% (wt/vol) PEG 8000 and 200 mmol/L NaCl. The mixture was incubated overnight at 4°C, followed by centrifugation at 3500*g* for 30 minutes. Pellets were suspended in Opti-MEM reduced serum medium (Invitrogen) to 1/100 of the original volume, and HBV DNA was extracted using an SMI TEST EX R&D Kit (MLB, Nagoya, Japan). HBV copies were detected by RTD-PCR. For the preparation of NL-HBV particles, the pUC1.2xHBV/NL and pUCxHBV-delta plasmids were provided by Professor Shimotohno (Research Center for Hepatitis and Immunology, National Center for Global Health and Medicine, Chiba, Japan) and co-transfected into HepG2 cells using Lipofectamine 3000 (Invitrogen). Cell culture supernatant was harvested at 5 and 7 days after transfection and filtered through 0.45-μm filter units. Harvested NL-HBV particles were treated by DNase I and used for infection. Viral particles were extracted from the supernatants of HepG2.2.15-HBV-CAT-TC155 cells or HepG2.2.15-HBV-CAT-TCPreS1 cells using a PEG Virus Precipitation Kit and labeled with a TC-ReAsH II In-Cell Tetracysteine Tag Detection Kit (Thermo Fisher Scientific). ReAsH-TC155HBV was tagged with tetracysteine (C-C-P-G-C-C) at the 155th capsid amino acid and labeled with the ReAsH fluorescent dye[15]; ReAsH-PreS1HBV virions tagged with tetracysteine in PreS1 were labeled with the ReAsH fluorescent dye. The HBV used to infect PXB cells was purchased from PhoenixBio Co, Ltd.

Establishment of Huh7-shDOCK11, HepG2-NTCP-C4-shDOCK11, and HepG2-NTCP-C4-RAB7KO Cell Lines

To establish the Huh7-shDOCK11 and HepG2-NTCP-C4-shDOCK11 cell lines, MISSION Lentiviral Packaging Mix (Sigma-Aldrich) was used to generate lentiviruses with an shRNA plasmid targeting DOCK11 in the Lenti-X 293T Cell Line (Takara Bio USA, Mountain View, CA). As a negative control, the pLKO.1 Puro Non-Target shRNA Control Plasmid was used. Huh7 and HepG2-NTCP-C4 cells were infected with medium containing the lentiviruses generated from Lenti-X 293T cells. At 20 hours after infection, the medium was replaced with fresh medium. At 3 days after infection, the cells were selected by 5 mg/mL puromycin (Thermo Fisher Scientific). All experiments were performed within 2 weeks after lentiviral transduction. To establish the HepG2-NTCP-C4 RAB7KO cell line, the target sequence of RAB7A was cloned into the lentiCRISPRv2 backbone (Addgene, Cambridge, MA). To make the lentiviruses, the plasmid (to clone the target sequences into the lentiCRISPRv2 backbone) was co-transfected into Lenti-X 293T cells (Takara Bio USA) with Packaging Mix (third generation mix from ABM). Harvested lentiviruses were transduced into HepG2-NTCP-C4 cells. At 3 days after transduction, these cells were treated with 5 mg/mL puromycin for 1 week. After puromycin selection, gene knockout of RAB7 was confirmed by immunoblotting and immunofluorescence analyses.

Establishment of the Dox-Inducible HepG2-NTCP-C4-Halo-DOCK11 Cell Line

The fragment of Halo-DOCK11 was digested from the pFN21A Halo-DOCK11 CMV Flexi vector (FHC29467) and inserted into the Retro-X Tet-On 3G vector, followed by the establishment of HepG2-NTCP-C4-Halo-DOCK11 stable cells according to the instructions of the Retro-X Tet-On 3G inducible expression system (Takara Bio USA).

Infection Model of HepG2-NTCP-C4–Derived Cells

HepG2-NTCP-C4-RAB7KO and control HepG2-NTCP-C4-ScrambleKO cells, HepG2-NTCP-C4-shDOCK11 and control HepG2-NTCP-C4-shScramble cells, and HepG2-NTCP-C4-

Figure 10. (***See previous page***). **DOCK11 and AGAP2 regulate ARF1 activity to promote the retrograde trafficking of HBV.** (*A* and *B*) Co-immunoprecipitation of DOCK11 and AGAP2 with ARF1 in HepG2-NTCP-C4 cells (Endogenous) (*A*) or HepG2-NTCP-C4-Halo-DOCK11 cells that were transfected with the Halo-AGAP2 plasmid and treated with Dox (Exogenous) (*B*). (*C*) A deletion mutant of DOCK11, DHR2-DOCK11-Flag, was constructed and confirmed using immunoblotting analysis. (*D* and *E*) HepG2-NTCP-C4 cells were transfected with DHR2-DOCK11-Flag or full-length Halo-DOCK11 and then infected with NL-HBV particles. HBV DNA (*D*) and cccDNA (*E*) levels were detected by RTD-PCR. (*F* and *G*) Measurement of GEF activity. GEF activity of titrated recombinant DOCK11 protein toward a fixed protein concentration of recombinant CDC42 (*F*) or ARF1 (*G*) using the GTPase-Glo Assay. (*H*) GAP activity of titrated recombinant AGAP2 protein toward a fixed protein concentration of recombinant ARF1 using the GTPase-Glo Assay. (*I* and *J*) RAB7KO or control cells were infected with NL-HBV particles with or without BFA treatment for 30 hours. HBV DNA (*I*) and cccDNA (*J*) levels were detected by RTD-PCR. (*K*) The Golgi fraction was isolated from both groups of cells, and HBV capsid antigen was measured by enzyme-linked immunosorbent assay. (*L* and *M*) HepG2-NTCP-C4 cells were infected with NL-HBV particles for 30 hours together with NAV-2729, an inhibitor of ARF1, at the indicated concentration. HBV DNA (*L*) and cccDNA (*M*) levels were measured by RTD-PCR. Representative results from 3 independent experiments are shown. $^{*}P < .05$, $^{**}P < .01$, $^{***}P < .001$, $^{****}P < .0001$. (*N*) Schematic representation of DOCK11-AGAP2-ARF1–mediated HBV retrograde trafficking via the EE-TGN-ER pathway to the nucleus.

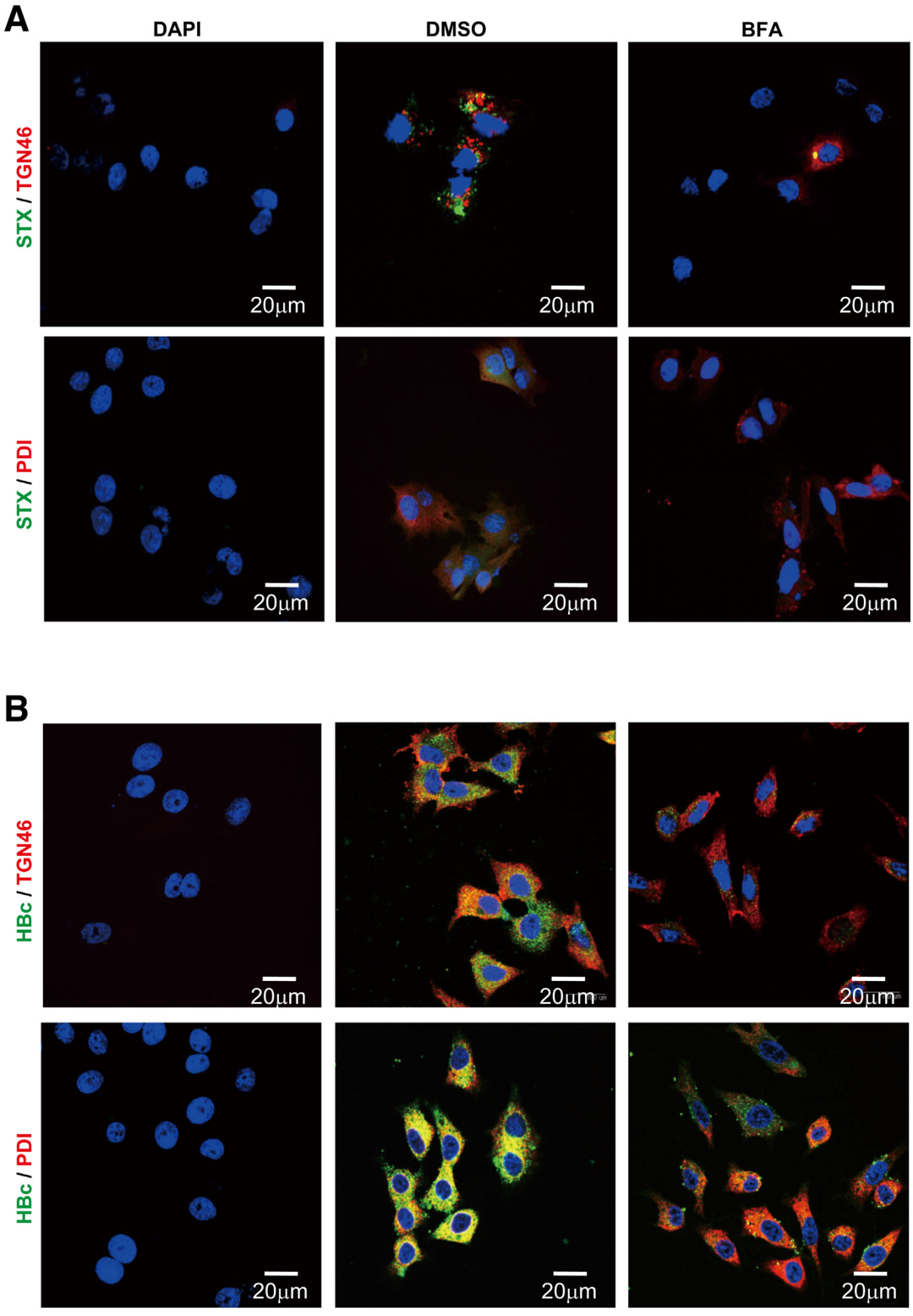

Figure 11. Immunofluorescence staining of STX or HBV capsid is found within TGN or ER organelles. RAB7KO cells were incubated with Alexa Fluor 532-labeled STX for 30 minutes (*A*) or NL-HBV virions for 120 minutes (*B*) with or without 2 μmol/L BFA. Immunofluorescence signals were analyzed by confocal microscopy. *Green signals* are STX or HBV capsids, and *red signals* are Golgi or ER. *Yellow signals* are co-localized signals. Scale bars, 20 μm.

Halo-DOCK11 cells were established from HepG2-NTCP-C4 cells as described below. These cells were infected with recombinant NL-HBV particles or HBV virions from HepAD38 cells at 6,000,000 genome equivalents (GEq)/cell in the presence of 4% PEG 8000 and 2% DMSO. For HBV DNA and cccDNA detection, the cells were infected with NL-

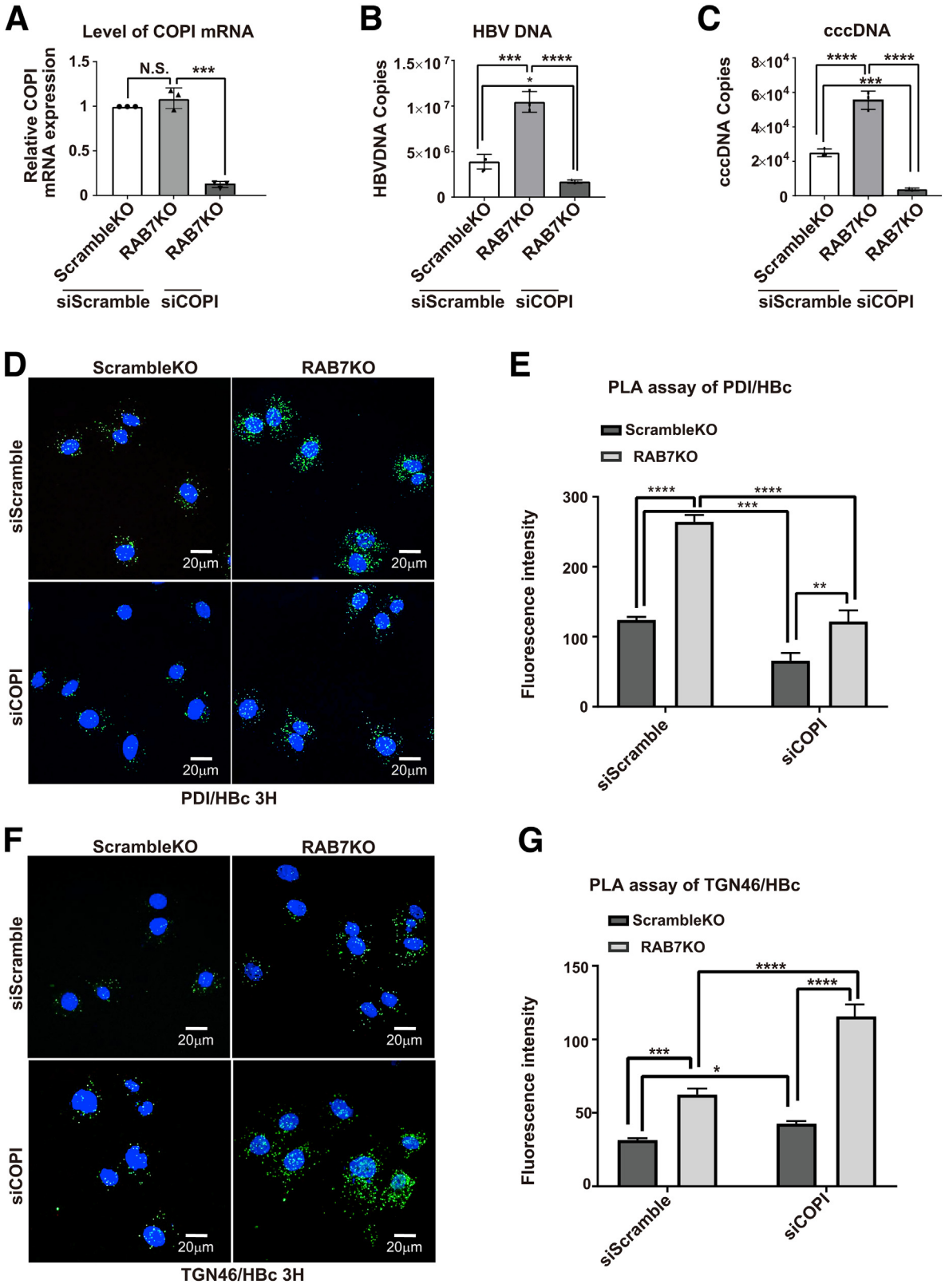

Figure 12. Depletion of COPI expression suppresses HBV DNA and cccDNA levels by inhibiting HBV capsid retrograde trafficking to the TGN or ER in RAB7KO cells infected with NL-HBV particles. (*A–C*) Cells were transfected with siCOPI or siScramble and then infected with NL-HBV particles. COPI mRNA (*A*), HBV DNA (*B*), and cccDNA (*C*) levels were detected by RTD-PCR. (*D–G*) Confocal images of PLA using rabbit anti-HBcAg and mouse anti-PDI (*D* and *E*) or anti-TGN46 (*F* and *G*) antibodies in COPI-silenced cells were compared with those from control siScramble transfected cells. Representative results from 3 independent experiments are shown. *$P < .05$, **$P < .01$, ***$P < .001$, ****$P < .0001$.

HBV virions for 30 hours. For the PLA or immunofluorescence analysis, the cells were infected with NL-HBV virions, ReAsH-TC155HBV, or ReAsH-PreS1HBV virions for 30, 60, 90, 120, and 180 minutes. For the HBcAg enzyme-linked immunosorbent assay and co-immunoprecipitation assay, the cells were infected with HBV virions from HepAD38

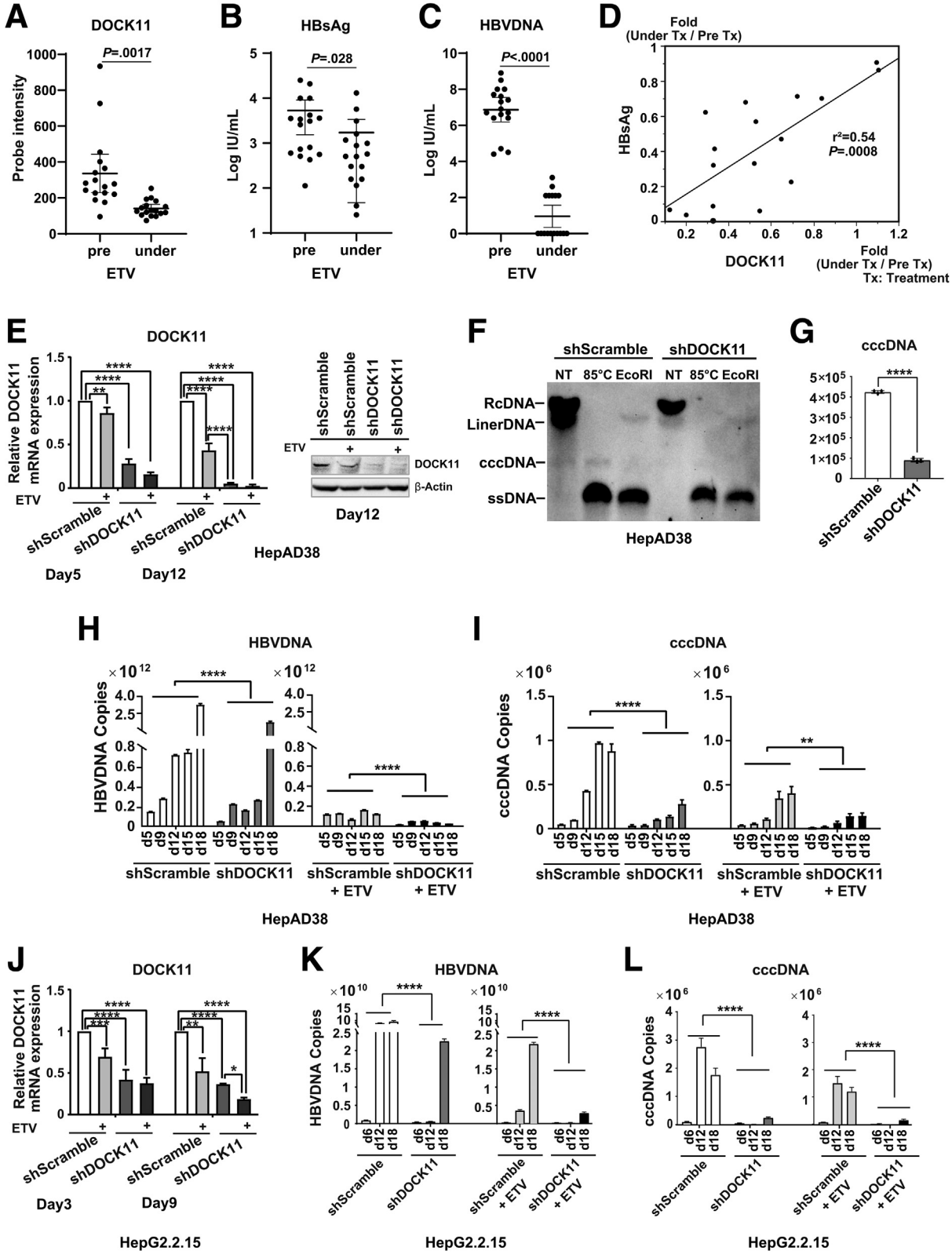

cells for 2 hours. In some experiments, at 1 day before infection with HBV virions, the cells were transfected with plasmid or siRNA or treated with Dox.

Infection Model of PXB Cells

As a comparison with HCC cells, freshly isolated hepatocytes from humanized chimeric mouse liver (PXB cells) were used to confirm the function of DOCK11. PXB cells in a special culture medium (#PPC-M200; PhoenixBio Co, Ltd) were infected with HBV particles (#PPC-BC; PhoenixBio Co, Ltd) at 5 GEq/cell in the presence of 4% PEG 8000 and 2% DMSO overnight. The following day, the medium was replaced with fresh medium and then changed every 4 days until day 24. At day 24, total RNA was collected, and DOCK11 mRNA levels were detected by RTD-PCR. In some experiments, PXB cells were infected with lentiviruses carrying shDOCK11, shAGAP2, or control Scramble shRNA. The following day, the medium was replaced with fresh medium. After 7 days, PXB cells were infected with HBV particles (PhoenixBio Co, Ltd) or HBV particles from HepAD38 cells overnight, and the medium was changed every 4 days until day 17. Total RNA and genomic DNA were collected. DOCK11, AGAP2, HBV DNA, and cccDNA were detected by RTD-PCR analysis or Southern blotting. In another experiment, original PXB cells were reseeded into 8-chamber slides. After 7 days, the cells were infected with HBV particles (PhoenixBio Co, Ltd) overnight, and fresh medium was added every 4 days until day 30. Immunofluorescence analysis was carried out using Alexa Fluor 488-labeled DOCK11 together with anti-TGN46, anti-GM130, or anti-HBcAg antibodies as the primary antibody. The secondary antibody was Alexa Fluor 594-conjugated anti-mouse immunoglobulin (Ig) G antibody. Images were captured with a Dragonfly high-speed confocal microscope (Andor, Oxford Instruments, Belfast, UK).

Hirt DNA Extraction and Southern Blot Analysis

The Hirt protein-free DNA extraction procedure was used to isolate cccDNA from HBV-infected cells or HepAD38 cells.[31] Full-length HBV was inserted into a pSPT19 vector to generate the pSPT19-HBV plasmid. The pSPT19-HBV template was linearized by *Bam*HI (Takara, Shiga, Japan), and in vitro transcription was performed with 1 μg linearized DNA template and a DIG RNA Labeling Kit (Roche, Basel, Switzerland) in the presence of T7 RNA polymerase to generate digoxigenin-UTP-labeled, single-stranded RNA probes. Hirt-extracted DNA was electrophoresed on 1.2% agarose gels and blotted onto a Hybond-N+ membrane (GE Healthcare, Amersham, UK). DIG-labeled single-stranded RNA probes transcribed from pSPT19-HBV plasmids were used to detect HBV cccDNA. Hybridization was performed with a 30-minute pre-hybridization at 50°C in 10 mL DIG Easy Hyb buffer (Roche) and with overnight hybridization at 50°C in 5 mL pre-warmed DIG Easy Hyb buffer containing 1 μg DIG-labeled probe (Roche). The membranes were washed with a Wash and Block Buffer Set (Roche). Probe-target hybrids were localized with 4 μL of anti-digoxigenin-AP conjugate (Roche) and detected by 1 mL CSPD (Roche). Images were acquired with the ChemiDoc Touch Imaging System (Bio-Rad, Hercules, CA).

Iodixanol Density Gradient Analysis

The medium from HepG2-HBV-CAT-TCPreS1 cells was harvested at 6, 8, and 10 days after plating. The virus fraction was precipitated using a PEG Virus Precipitation Kit (BioVision, Milpitas, CA). After determining HBV DNA levels by RTD-PCR, 2.8×10^9 copies of HBV DNA were layered on a 10%–40% iodixanol gradient and centrifuged at 178,000*g* for 21 hours at 4ºC in an SW41Ti rotor. Fractions were collected from the top of the gradient, and the density and HBsAg, HBcrAg, and HBV DNA levels were measured in each fraction. HepG2-NTCP-C4 cells were infected with fractions 17 and 18, and fluorescence microscopy images were captured with an HM-1000 super-resolution microscope (Sysmex Corp, Kobe, Japan) and Dragonfly confocal microscope (Andor, Oxford Instruments).

Super-Resolution Fluorescence Microscopy

HepG2-NTCP-C4 cells were seeded at a density of 1.0×10^4 cells/mL in Nunc Lab-Tek chamber slides (Capitol Scientific, Austin, TX) and incubated with a baculovirus infection system encoding GFP-fused RAB5A, GFP-fused RAB7A, and CellLight Golgi-GFP BacMam 2.0 (Thermo Fisher Scientific) overnight at 37°C in a 5% CO_2 atmosphere. The next day, the medium was replaced with fresh medium containing Hoechst 33342 (Thermo Fisher Scientific) for another 30 minutes. The medium was replaced by fresh growth medium containing ReAsH-labeled TC155HBV particles or ReAsH-labeled TCPreS1HBV particles purified by iodixanol density gradient. At the indicated times, the cells were fixed in 4% paraformaldehyde. Images were captured with an HM-1000

Figure 13. (***See previous page***). **DOCK11 expression is associated with ETV treatment *in vivo* and *in vitro*.** (*A*) DOCK11 expression in biopsied liver tissues of CHB patients. (*B* and *C*) Changes of HBsAg (*B*) and HBV DNA (*C*) levels in the serum of CHB patients before and after ETV treatment. (*D*) Spearman's correlation analysis of the reduction rate of DOCK11 with that of HBsAg in CHB patients before and after ETV treatment. (*E*) DOCK11 stable knocked-down HepAD38-shDOCK11 cells and negative control cells were treated with 2.5 nmol/L ETV. Samples were collected at the indicated time points. Endogenous DOCK11 expression was detected by RTD-PCR (*left*) and immunoblotting (*right*). (*F*) Hirt-extracted HBV DNA was detected by Southern blotting under the condition of no treatment, 85°C for 5 minutes, or 85°C for 5 minutes plus *Eco*RI digestion for 16 hours at day 10. (*G*) cccDNA levels in genomic DNA were detected by RTD-PCR. (*H* and *I*) The above cells were treated with or without 2.5 nmol/L ETV and collected at the indicated time points. HBV DNA (*H*) and cccDNA (*I*) levels were detected by RTD-PCR. (*J–L*) DOCK11 stable knocked-down HepG2.2.15-shDOCK11 cells and control cells were treated with 2.5 nmol/L ETV. Samples were collected at the indicated time points. DOCK11 (*J*), HBV DNA (*K*), and cccDNA (*L*) levels were detected by RTD-PCR. Representative results from 3 independent experiments are shown. $^*P < .05$, $^{**}P < .01$, $^{***}P < .001$, $^{****}P < .0001$.

Table 1. Key Resources

Reagent or resource	Source	Identifier
Antibodies		
Mouse monoclonal Anti-HaloTag	Promega	Cat# G9211, RRID:AB_2688011
Rabbit polyclonal Anti-GFP	Medical Biological Laboratories	Cat# 598, RRID:AB_591819
Mouse monoclonal Anti-PDI	Abcam	Cat# ab2792
Mouse monoclonal Anti-TGN46	Abcam	Cat# ab2809, RRID:AB_2203290
Rabbit monoclonal Anti-RAB7	Cell Signaling Technology	Cat# 9367, RRID:AB_1904103
Mouse monoclonal Anti-RAB9	Abcam	Cat# ab2810, RRID:AB_303323
Rabbit polyclonal Anti-RAB11	Abcam	Cat# ab3612, RRID:AB_10861613
Mouse monoclonal Anti-RAB5	Santa Cruz Biotechnology	Cat# sc-46692, RRID:AB_628191
DOCK11 Antibody	Bethyl	Cat# A301-638A, RRID:AB_1210940
DOCK11 Antibody	Invitrogen	Cat# PA5-37152
Goat anti-Mouse IgG (H+L) Highly Cross-Adsorbed Secondary Antibody, Alexa Fluor Plus 488	Thermo Fisher Scientific	Cat# A32723TR, RRID:AB_2866489
Goat anti-Rabbit IgG (H+L) Highly Cross-Adsorbed Secondary Antibody, Alexa Fluor Plus 594	Thermo Fisher Scientific	Cat# A32740, RRID:AB_2762824
Normal Rabbit IgG antibody	Cell Signaling Technology	Cat# 2729, RRID:AB_1031062
DYKDDDDK Tag Antibody	Cell Signaling Technology	Cat# 2368, RRID:AB_2217020
Anti-Hepatitis B Virus Core Antigen antibody	Abcam	Cat# ab8637, RRID:AB_306684
Anti-HBcAg Polyclonal Antibody	Beacle	Cat#BCL-ABPC-01
Anti-Hepatitis B virus Core antigen antibody	Abcam	Cat# ab115992
Anti-ARF1 antibody	Abcam	Cat# 183576
Rabbit monoclonal anti-b-actin	Cell Signaling Technology	Cat# 8457, RRID:AB_10950489
Anti-rabbit IgG, HRP-linked Antibody	Cell Signaling Technology	Cat# 7074, RRID:AB_2099233
Anti-mouse IgG, HRP-linked Antibody	Cell Signaling Technology	Cat# 7076, RRID:AB_330924
CellLight Golgi-GFP, BacMam 2.0	Thermo Fisher Scientific	Cat# C10592
CellLight ER-GFP, BacMam 2.0	Thermo Fisher Scientific	Cat# C10590
Mouse monoclonal Anti-GS28 (F-11)	Santa Cruz Biotechnology	Cat# sc-271551
Anti-PIKE antibody	Abcam	Cat# ab224118
PIKE Polyclonal Antibody	Bethyl	A304-262A
Bacterial and **v**irus **s**trains		
Subcloning Efficiency DH5a Competent Cells	Thermo Fisher Scientific	Cat# 18265017
HBV Genotype C Strain	This article	Purified from HepG2.2.15 or HepAD38
HBV-TcPreS1 Genotype C strain	This article	Purified from HepG2-TcPreS1
HBV-Tc155 Genotype C strain	This article	Purified from HepG2-Tc155
HBV-Nano-Luc Genotype C strain	Professor Nishitsuji	N/A
Chemicals, peptides, and recombinant proteins		
Brefeldin A	Sigma-Aldrich	Cat# B5936
Dynasore hydrate	Sigma-Aldrich	Cat# D7693
Pitstop2	Sigma-Aldrich	Cat# SML1169
Retro2	Sigma-Aldrich	Cat# SML1085
E-64d protease inhibitor	Sigma-Aldrich	Cat# E8640-1MG
Bafilomycin A1 Ready Made Solution	Sigma-Aldrich	Cat# SML1661-.1ML
Chloroquine	Sigma-Aldrich	Cat# C6628
NH4Cl	Sigma-Aldrich	Cat# A9434
NAV-2729	Sigma-Aldrich	Cat# SML2238-5MG
CDC42 (Human) Recombinant Protein (P01)	Abnova	H00000998-P01
ARF1 (Human) Recombinant Protein (P01)	Abnova	H00000375-P01
AGAP2 (Human) Recombinant Protein (P01)	Abnova	H00116986-P01
Recombinant protein of DHR2-DOCK11-Flag	Professor Matsushima	N/A
Critical **c**ommercial assays		
Duolink In Situ PLA Probe Anti-Mouse PLUS	Sigma-Aldrich	DUO92001-100RXN
Duolink In Situ PLA Probe Anti-Rabbit MINUS	Sigma-Aldrich	DUO92005-100RXN
Duolink In Situ Detection Reagents Green	Sigma-Aldrich	DUO92014-100RXN
Duolink In Situ Wash Buffers, Fluorescence	Sigma-Aldrich	DUO82049-4L
Protein G Mag Sepharose	GE Healthcare	28951379
CDC42 Activation Assay Kit	Cell Biolabs, Inc	STA-402
Arf1 Activation Assay Kit	Cell Biolabs, Inc	STA-407-1
HBV Core antigen/HBcAg ELISA Kit	Arigo Biolaboratories	ARG82006
Nano-Glo Luciferase Assay Kit	Promega	Cat# N1120
Golgi Isolation Kit	Sigma-Aldrich	Cat# GL0010
GeneArt Genomic Cleavage Detection Kit	Invitrogen	Cat# A24372
OptiPrep Density Gradient Medium	Sigma-Aldrich	Cat# D1556
PEG Virus Precipitation Kit	Bio Vision	Cat# K904-200-1
Experimental models: cell lines		
HepG2.2.15	Lab stored	N/A
HepAD38	Lab stored	N/A
HepG2-NTCP-C4	Lab stored	N/A
HepG2	Lab stored	N/A
Huh7	Lab stored	N/A
PXB cells	PhoenixBio	N/A

Table 1. Continued

Reagent or resource	Source	Identifier
HepG2-HBV-CAT-TCPreS1	Lab stored	N/A
HepG2-HBV-CAT-TC155	Lab stored	N/A
HepG2-NTCP-C4-Scramble KO	This article	N/A
HepG2-NTCP-C4-RAB7 KO	This article	N/A
HepG2-NTCP-C4-Halo-DOCK11	This article	N/A
Huh7-shScramble	This article	N/A
Huh7-shDOCK11	This article	N/A
HepAD38-shScramble	Lab stored	N/A
HepAD38-shDOCK11	This article	N/A
HepG2.2.15-shScramble	This article	N/A
HepG2.2.15-shDOCK11	This article	N/A
Biological samples		
Liver biopsy samples	Kanazawa University Graduate School of Medicine	N/A
Serum samples	Kanazawa University Graduate School of Medicine	N/A
Recombinant DNA		
AGAP2 (Flexi Halo Tag Type)	Promega	FHC00439
DOCK11 (Flexi Halo Tag Type)	Promega	FHC29467
GFP-DOCK11-pcDNA3.3	This article	N/A
pLKO.1-puro Non-Mammalian shRNA Control Plasmid DNA	Sigma-Aldrich	Cat #SHC002
pLKO.1-puro-shDOCK11	Sigma-Aldrich	SHCLND-NM_144658; TRCN0000376430
LentiCRISPRv2	Addgene	Cat# 52961
LentiCRISPRv2 sgControl	This article	N/A
LentiCRISPRv2 sgRAB7A	This article	N/A
AGAP2-Flag-pcDNA3.1	This article	N/A
pCMV-Srript EX-HBV-pgRNA	This article	N/A
TrueGuide Synthetic DOCK11 gRNA	Invitrogen	CRISPR800769-CR
DOCK11-DHR2-Flag-pcDNA3.1	This article	N/A
Software and algorithms		
GraphPad Prism	GraphPad	https://www.graphpad.com/scientific-software/prism/
ImageJ	ImageJ	https://imagej.nih.gov/ij/

super-resolution microscope (Sysmex Corp) and Dragonfly confocal microscope (Andor, Oxford Instruments).

Live Cell Confocal Imaging

The cells were seeded at a density of 1.0×10^4 cells/mL in chamber slides and incubated with CellLight Golgi-GFP BacMam 2.0 or CellLight ER-GFP BacMam 2.0 overnight at 37°C in a 5% CO_2 atmosphere. The next day, the medium was replaced with fresh growth medium containing Hoechst 33342 for another 30 minutes. Then, the medium was replaced with fresh growth medium containing ReAsH-labeled TC155HBV particles. Time-lapse fluorescence images of ReAsH-labeled TC155HBV particles were acquired every 1 minute for up to 180 minutes (180 frames) using an LSM510 inverted confocal microscope (Zeiss, Jena, Germany).

Constructs and Transfection of Plasmids

The Halo-DOCK11 (FHC29467) and Halo-AGAP2 (FHC24787) plasmids were purchased from the Kazusa DNA Research Institute (Chiba, Japan). The plasmid constructs for AGAP2-Flag and DHR2-DOCK11-Flag were cloned into pcDNA3.1 using the primer sets shown in Table 2. Transfections were performed with Lipofectamine 3000 (Invitrogen).

Dynasore, Pitstop 2, Retro-2, BFA, and NAV-2729 Treatment of HepG2-NTCP-C4 or RAB7KO Cells Infected With Recombinant NL-HBV Particles

HepG2-NTCP-C4 cells transfected with Halo-DOCK11 or HepG2-NTCP-C4 RAB7KO cells were infected with recombinant NL-HBV particles or HBV from HepAD38 cells at 6,000,000 GEq/cell with or without Dynasore, Pitstop 2, Retro-2, BFA, or NAV-2729 at the indicated concentrations. All infections were performed in the presence of 4% PEG 8000 and 2% DMSO at 37°C for 30 hours. After the cells were washed with phosphate-buffered saline (PBS), cell lysate and genomic DNA were collected. HBV DNA and cccDNA levels were determined by RTD-PCR, and Luc fluorescence was detected by a Nano-Glo Luciferase Assay Kit (Promega, Madison, WI).

Lysosome Inhibitor Treatment of HepG2-NTCP-C4 Cells Infected With Recombinant NL-HBV Particles

HepG2-NTCP-C4 cells were infected with recombinant NL-HBV particles at 60,000 GEq/cell with or without

Table 2. Oligonucleotides for shRNA, CRISPR/Cas9, Cloning, and RTD-PCR

Name	Sequence (5′–3′)	Note
pLKO.1-puro non-mammalian shRNA control plasmid DNA	CCGGCAACAAGATGAAGAGCACCAACTCGAGTTG GTGCTCTTCATCTTGTTGTTTTT	Insert sequence of shRNA
pLKO.1-puro-shDOCK11	CCGGTGATGGCCATAACCCATTAATCTCGAGATTA ATGGGTTATGGCCATCATTTTTG	Insert sequence of shRNA
Human non-targeting control sgRNA forward	CACCGCACTCACATCGCTACATGA	sgRNA for CRISPR/Cas9 non-targeting control
Human non-targeting control sgRNA reverse	AAACTCATGTAGCGATGTGAGTGC	sgRNA for CRISPR/Cas9 non-targeting control
Human non-targeting RAB7A sgRNA forward	CACCGAGGCGTTCCAGACGATTGCA	sgRNA for CRISPR/Cas9-mediated human Rab7A editing
Human non-targeting RAB7A sgRNA reverse	AAACTGCAATCGTCTGGAACGCCTC	sgRNA for CRISPR/Cas9-mediated human Rab7A editing
AGAP2-Flag-pcDNA3.1 forward	TAAGGTACCATGAGCCGGGGCGCGGGCGC	Cloning primer
AGAP2-Flag-pcDNA3.1 reverse	AATTCTAGATTACTTGTCATCGTCATCCTTGTAGTC TACCAGCGCAACCGGGGCGT	Cloning primer
DOCK11-DHR2-Flag-pcDNA3.1 forward	TAAGGTACCGCCGCCATGGTAGCACTAA GCGGAGGAT	Cloning primer
DOCK11-DHR2-Flag-pcDNA3.1 reverse	AATTCTAGATTACTTGTCATCGTCATCCTTGTA GTCCACTTCAGCGTATC	Cloning primer
cccDNA for RTD-PCR forward	CGTCTGTGCCTTCTCATCTGC	Detection of cccDNA levels
cccDNA for RTD-PCR reverse	GCACAGCTTGGAGGCTTGAA	Detection of cccDNA levels
HBV DNA for RTD-PCR forward	ACTCACCAACCTCCTGTCCT	Detection of HBV DNA levels
HBV DNA for RTD-PCR reverse	GACAAACGGGCAACATACCT	Detection of HBV DNA levels

lysosome inhibitors (Sigma-Aldrich) including E46d, Baf1, chloroquine, or NH_4Cl at the indicated concentrations. All infections were performed in the presence of 4% PEG 8000 and 2% DMSO at 37°C for 30 hours. After the cells were washed with PBS, the cell lysate and genomic DNA were collected. HBV DNA levels were determined by RTD-PCR. Cell density was evaluated using a Cell Counting Kit-8 (Dojindo, Kumamoto, Japan).

Establishment of the HepAD38-shDOCK11 and HepG2.2.15-shDOCK11 Cell Lines

MISSION Lentiviral Packaging Mix (Sigma-Aldrich) was used to generate lentiviruses with an shRNA plasmid targeting DOCK11 in Lenti-X 293T cells (Takara Bio USA). As a negative control, the pLKO.1 Puro Non-Target shRNA Control Plasmid was used. HepAD38 and HepG2.2.15 cells were infected with medium containing the lentiviruses generated from Lenti-X 293T cells. At 24 hours after infection, the medium was replaced with fresh medium. At 3 days after infection, the cells were selected by 8 mg/mL puromycin (Thermo Fisher Scientific).

Immunofluorescence Analysis

The cells were seeded at 1.0×10^5 cells/well in a 4-chamber slide, and after 16–18 hours, they were transfected with the GFP-DOCK11 plasmid or treated with Dox for HepG2-NTCP-C4-Halo-DOCK11 cells. At 48 hours after transfection, the cells were washed 3 times with PBS and fixed in 4% paraformaldehyde for 10 minutes at room temperature. After washing with PBS-T, the cells were permeabilized with PBS containing 0.5% Triton X-100, incubated in a blocking solution (X0909; Dako, Santa Clara, CA) for 30 minutes, and reacted with an anti-GFP antibody (cat. no. 598; Medical and Biological Lab Co, Ltd, Aichi, Japan) and Alexa Fluor 555-labeled DOCK11 as the primary antibody for 1 hour. The secondary antibody was Alexa Fluor 488-conjugated anti-rabbit Ig G antibody for GFP. The cells were mounted with mounting medium containing DAPI (Vector Laboratories, Burlingame, CA). Imaging was performed with a CSU-X1 confocal microscope (Yokogawa Electric Corporation, Tokyo, Japan). In some experiments, HepG2-NTCP-C4 RAB7KO cells were seeded at 2.0×10^4 cells/well in an 8-chamber slide, and at 16–18 hours later, the cells were infected with NL-HBV particles. At the indicated times, the cells were fixed in 4% paraformaldehyde. Images were captured with a Dragonfly high-speed confocal microscope (Andor, Oxford Instruments).

PLA

To visualize the close proximity of HBcAg and EEs, TGN, or ER, HepG2-NTCP-C4 or HepG2-NTCP-C4-RAB7KO cells were infected with NL-HBV particles at a multiplicity of infection of 6,000,000 and incubated for the indicated times before fixation with 4% paraformaldehyde. After fixation, the cells were permeabilized with PBS containing 0.5% Triton X-100 and then incubated in a blocking solution (X0909; Dako) for 30 minutes. The cells were stained for HBcAg (1:100 dilution), RAB5 (1:100 dilution), TGN46 (1:50 dilution), or PDI (1:100 dilution) by overnight incubation at 4°C. These cells were immunostained using the PLA (Sigma-Aldrich). The cells

were washed, and the nuclei were counterstained with DAPI. Fluorescence micrographs were collected by confocal microscopy. Fluorescent foci were quantified using ImageJ software (available from http://rsb.info.nih.gov/ij/). Threshold levels were set using a PLA-processed sample without primary antibodies in each staining group.

Extraction of the Golgi Fraction

The Golgi fraction was extracted from cultured cells using a Golgi Isolation Kit (Sigma-Aldrich). The Golgi fraction was verified by immunoblotting with a rabbit anti-human GS28 antibody. For the HBcAg enzyme-linked immunosorbent assay, HepG2-NTCP-C4 RAB7KO cells were treated with BFA at 30 minutes before infection and then replacement with fresh medium containing NL-HBV virions, 4% PEG 8000, 2% DMSO, and 2 μmol/L BFA. After infection for 2 hours and BFA treatment, the cells were harvested, and the Golgi fraction was extracted.

HBcAg Enzyme-Linked Immunosorbent Assay

The HepG2-NTCP-C4-ScrambleKO and HepG2-NTCP-C4-RAB7KO cell lines were infected with HBV particles purified from the HepAD38 cell line. After infection for 3 hours, the Golgi fraction was isolated (GL0010; Sigma-Aldrich). HBcAg protein levels were measured by a commercial enzyme-linked immunosorbent assay kit (ARG82006; Arigo, Taiwan, China).

Immunoblotting Analysis

Immunoblotting analysis was performed as described previously.[32] Protein extracts were prepared with RIPA Lysis Buffer (Merck Millipore, Burlington, MA) containing Protease Inhibitor Cocktail and Phosphatase Inhibitor Tablets (Roche Applied Science, Pleasanton, CA). Halo-DOCK11, RAB7, RAB5, RAB9, RAB11, AGAP2-Flag, ARF1, and β-actin expression was evaluated with mouse anti-Halo (Promega), rabbit anti-RAB7, -RAB5, -RAB9, and -RAB11, rabbit anti-Flag, rabbit anti-ARF1, and rabbit anti-β-actin antibodies (Cell Signaling Technology, Danvers, MA), respectively.

Immunoprecipitation Assay

Cell lysates were incubated with rabbit IgG or rabbit anti-DOCK11, anti-ARF1, or anti-Flag antibodies overnight at 4°C. Immunoprecipitation was performed using Protein G Mag Sepharose (GE Healthcare, Little Chalfont, UK). The beads were washed in lysis buffer and eluted in sodium dodecyl sulfate sample buffer. The reaction mixtures were analyzed by immunoblotting.

Quantification of HBV DNA and cccDNA by RTD-PCR

HBV DNA was extracted from the cells using a DNeasy Blood & Tissue Kit (QIAGEN, Valencia, CA). The extracted DNA (250 ng) was treated for 30 minutes at 37°C with 25 U T5 Exonuclease (New England BioLabs, Ipswich, MA) and treated for 5 minutes at 95°C for enzyme heat inactivation. HBV DNA and cccDNA levels were quantified with qPCR MasterMix Plus Low ROX (Nippon Gene, Tokyo, Japan) using a specific HBV DNA probe (5′-FAM/TATCGCTGG/ZEN/ATGTGTCTGCGGCGT/3IBFQ-3′) and cccDNA probe (5′-FAM-CTGTAGGCATAAATTGGT-MGB-3′). HBV DNA and cccDNA primer sets are shown in Table 2.

RNA Extraction and RTD-PCR Analysis

Total RNA was isolated using a NIPPON Cell & Tissue RNA Kit (Nippon Gene). A High-Capacity cDNA Reverse Transcription Kit (Thermo Fisher Scientific) was used for first-strand cDNA synthesis with 0.2 μg total RNA from each sample. RTD-PCR was conducted using TaqMan Gene Expression Assay Identification. Quantitative gene expression data were normalized to the expression levels of the housekeeping gene GAPDH (Thermo Fisher Scientific).

Recombinant Proteins

Recombinant DOCK11-DHR2-Flag (containing residues 4678–6285 of DOCK11) was provided by Professor Matsushima (Tokyo University); ARF1, AGAP2, and CDC42 proteins were obtained from Abnova (Taiwan, China).

GEF and GAP Activity Assays in Vitro

GEF and GAP activity assays were performed using a GTPase-Glo Assay Kit (Promega). Briefly, for in vitro GEF activity assays, we prepared a 2× GTPase-GAP solution containing 1 mmol/L DTT and a fixed amount of ARF1 or CDC42 and serially diluted DOCK11 as a GEFase at twice the desired final concentration in GEF buffer (50 mmol/L Tris-HCl, pH 7.5, 50 mmol/L NaCl, 1 mmol/L EDTA, and 10 mmol/L $MgCl_2$). For in vitro GAP activity assays, we prepared a 2× GTPase solution containing 1 mmol/L DTT and a fixed amount of ARF1 and serially diluted AGAP2 as a GAP at twice the desired final concentration in GTPase/GAP buffer (50 mmol/L Tris-HCl, pH 7.5, 50 mmol/L NaCl, 20 mmol/L EDTA, and 5 mmol/L $MgCl_2$). Both reaction solutions were added to an equal volume of GTPase-Glo reagent containing an enzyme to convert the GTP remaining after the GTPase reaction to ATP. The ATP generated in the reaction was detected by a luciferase/luciferin-based reagent. GAP and GEF activity was inversely correlated to the amount of light produced.

Statistical Analysis

All data are presented as the mean ± standard deviation. Experiments were repeated at least 3 times. Two-tailed unpaired Student t test or one-way analysis of variance was used to evaluate the data. Pearson's and Manders' correlation coefficients were used to assess colocalization. Spearman's correlation analysis was used to determine the correlation of the reduction rate of HBsAg and DOCK11. GraphPad Prism 7 software (version 17.0; IBM Corp., Armonk, NY) was used for data analysis. Statistical differences were considered significant at $P < .05$.

References

1. Cox AL, El-Sayed MH, Kao JH, Lazarus JV, Lemoine M, Lok AS, Zoulim F. Progress towards elimination goals for

viral hepatitis. Nat Rev Gastroenterol Hepatol 2020; 17:533–542.
2. Hashimoto S, Shirasaki T, Yamashita T, Iwabuchi S, Suzuki Y, Takamura Y, Ukita Y, Deshimaru S, Okayama T, Ikeo K, Kuroki K, Kawaguchi K, Mizukoshi E, Matsushima K, Honda M, Kaneko S. DOCK11 and DENND2A play pivotal roles in the maintenance of hepatitis B virus in host cells. PLoS One 2021;16:e0246313.
3. Laurin M, Cote JF. Insights into the biological functions of Dock family guanine nucleotide exchange factors. Genes Dev 2014;28:533–547.
4. Hasegawa H, Kiyokawa E, Tanaka S, Nagashima K, Gotoh N, Shibuya M, Kurata T, Matsuda M. DOCK180, a major CRK-binding protein, alters cell morphology upon translocation to the cell membrane. Mol Cell Biol 1996; 16:1770–1776.
5. He M, Westerberg LS. Congenital defects in actin dynamics of germinal center B cells. Front Immunol 2019;10:296.
6. Lin Q, Yang W, Baird D, Feng Q, Cerione RA. Identification of a DOCK180-related guanine nucleotide exchange factor that is capable of mediating a positive feedback activation of Cdc42. J Biol Chem 2006; 281:35253–35262.
7. Farhan H, Hsu VW. Cdc42 and cellular polarity: emerging roles at the Golgi. Trends Cell Biol 2016;26:241–248.
8. Yan H, Zhong G, Xu G, He W, Jing Z, Gao Z, Huang Y, Qi Y, Peng B, Wang H, Fu L, Song M, Chen P, Gao W, Ren B, Sun Y, Cai T, Feng X, Sui J, Li W. Sodium taurocholate cotransporting polypeptide is a functional receptor for human hepatitis B and D virus. Elife 2012;1:e00049.
9. Macovei A, Petrareanu C, Lazar C, Florian P, Branza-Nichita N. Regulation of hepatitis B virus infection by Rab5, Rab7, and the endolysosomal compartment. J Virol 2013;87:6415–6427.
10. Zhang W, Kazakov T, Popa A, DiMaio D. Vesicular trafficking of incoming human papillomavirus 16 to the Golgi apparatus and endoplasmic reticulum requires gamma-secretase activity. mBio 2014;5:e01777-14.
11. Iwamoto M, Watashi K, Tsukuda S, Aly HH, Fukasawa M, Fujimoto A, Suzuki R, Aizaki H, Ito T, Koiwai O, Kusuhara H, Wakita T. Evaluation and identification of hepatitis B virus entry inhibitors using HepG2 cells overexpressing a membrane transporter NTCP. Biochem Biophys Res Commun 2014;443:808–813.
12. Nishitsuji H, Ujino S, Shimizu Y, Harada K, Zhang J, Sugiyama M, Mizokami M, Shimotohno K. Novel reporter system to monitor early stages of the hepatitis B virus life cycle. Cancer Sci 2015;106:1616–1624.
13. Mercer J, Greber UF. Virus interactions with endocytic pathways in macrophages and dendritic cells. Trends Microbiol 2013;21:380–388.
14. Herrscher C, Roingeard P, Blanchard E. Hepatitis B virus entry into cells. Cells 2020;9.
15. Sun S, Yan J, Xia C, Lin Y, Jiang X, Liu H, Ren H, Yan J, Lin J, He X. Visualizing hepatitis B virus with biarsenical labelling in living cells. Liver Int 2014;34:1532–1542.
16. Shiba Y, Romer W, Mardones GA, Burgos PV, Lamaze C, Johannes L. AGAP2 regulates retrograde transport between early endosomes and the TGN. J Cell Sci 2010; 123(Pt 14):2381–2390.
17. Donaldson JG, Jackson CL. ARF family G proteins and their regulators: roles in membrane transport, development and disease. Nat Rev Mol Cell Biol 2011;12:362–375.
18. Nie Z, Fei J, Premont RT, Randazzo PA. The Arf GAPs AGAP1 and AGAP2 distinguish between the adaptor protein complexes AP-1 and AP-3. J Cell Sci 2005; 118(Pt 15):3555–3566.
19. Spang A, Shiba Y, Randazzo PA. Arf GAPs: gatekeepers of vesicle generation. FEBS Lett 2010;584:2646–2651.
20. Luna A, Matas OB, Martinez-Menarguez JA, Mato E, Duran JM, Ballesta J, Way M, Egea G. Regulation of protein transport from the Golgi complex to the endoplasmic reticulum by CDC42 and N-WASP. Mol Biol Cell 2002;13:866–879.
21. Park SY, Yang JS, Schmider AB, Soberman RJ, Hsu VW. Coordinated regulation of bidirectional COPI transport at the Golgi by CDC42. Nature 2015;521:529–532.
22. Kartberg F, Asp L, Dejgaard SY, Smedh M, Fernandez-Rodriguez J, Nilsson T, Presley JF. ARFGAP2 and ARFGAP3 are essential for COPI coat assembly on the Golgi membrane of living cells. J Biol Chem 2010; 285:36709–36720.
23. Hagelstein J, Fathinejad F, Stremmel W, Galle PR. pH-independent uptake of hepatitis B virus in primary human hepatocytes. Virology 1997;229:292–294.
24. Stoeckl L, Funk A, Kopitzki A, Brandenburg B, Oess S, Will H, Sirma H, Hildt E. Identification of a structural motif crucial for infectivity of hepatitis B viruses. Proc Natl Acad Sci U S A 2006;103:6730–6734.
25. Rigg RJ, Schaller H. Duck hepatitis B virus infection of hepatocytes is not dependent on low pH. J Virol 1992; 66:2829–2836.
26. Kuroki K, Eng F, Ishikawa T, Turck C, Harada F, Ganem D. gp180, a host cell glycoprotein that binds duck hepatitis B virus particles, is encoded by a member of the carboxypeptidase gene family. J Biol Chem 1995;270:15022–15028.
27. Tong Y, Tong S, Zhao X, Wang J, Jun J, Park J, Wands J, Li J. Initiation of duck hepatitis B virus infection requires cleavage by a furin-like protease. J Virol 2010; 84:4569–4578.
28. Soltysik K, Ohsaki Y, Tatematsu T, Cheng J, Fujimoto T. Nuclear lipid droplets derive from a lipoprotein precursor and regulate phosphatidylcholine synthesis. Nat Commun 2019;10:473.
29. Rabe B, Glebe D, Kann M. Lipid-mediated introduction of hepatitis B virus capsids into nonsusceptible cells allows highly efficient replication and facilitates the study of early infection events. J Virol 2006;80:5465–5473.
30. Ide M, Tabata N, Yonemura Y, Shirasaki T, Murai K, Wang Y, Ishida A, Okada H, Honda M, Kaneko S, Doi N, Ito S, Yanagawa H. Guanine nucleotide exchange factor DOCK11-binding peptide fused with a single chain antibody inhibits hepatitis B virus infection and replication. J Biol Chem 2022;298:102097.
31. Cai D, Nie H, Yan R, Guo JT, Block TM, Guo H. A southern blot assay for detection of hepatitis B virus covalently closed circular DNA from cell cultures. Methods Mol Biol 2013;1030:151–161.
32. Murai K, Honda M, Shirasaki T, Shimakami T, Omura H, Misu H, Kita Y, Takeshita Y, Ishii KA,

Takamura T, Urabe T, Shimizu R, Okada H, Yamashita T, Sakai Y, Kaneko S. Induction of selenoprotein P mRNA during hepatitis C virus infection inhibits RIG-I-mediated antiviral immunity. Cell Host Microbe 2019;25:588–601 e7.

Received December 24, 2021. Accepted October 12, 2022.

Correspondence
Address correspondence to: Masao Honda, MD, PhD, Department of Clinical Laboratory Medicine, Graduate School of Medical Science, Kanazawa University, Kodatsuno 5-11-80, Kanazawa, 920-0942, Japan. e-mail: mhonda@m-kanazawa.jp.

Acknowledgments
The authors thank Professor Yasuhito Tanaka, Department of Gastroenterology, Kumamoto University, for providing the HBV/C vectors and Dr Koichi Watashi, NIH, Japan, for providing the HepG2-NTCP-C4 cells.

CRediT Authorship Contributions
Ying-Yi Li (Data curation: Lead)
Kazuyuki Kuroki (Data curation: Supporting)
Tetsuro Shimakami (Data curation: Supporting)
Kazuhisa Murai (Data curation: Supporting)
Kazunori Kawaguchi (Data curation: Supporting)
Takayoshi Shirasaki (Investigation: Supporting)
Kouki Nio (Data curation: Supporting)
Saiho Sugimoto (Data curation: Supporting)
Tomoki Nishikawa (Data curation: Supporting)
Hikari Okada (Data curation: Supporting)
Noriaki Orita (Data curation: Supporting)
Hideo Takayama (Data curation: Supporting)
Ying Wang (Data curation: Supporting)
Phuong Doan Thi Bich (Data curation: Supporting)
Astuya Ishida (Data curation: Supporting)
Sadahiro Iwabuchi (Methodology: Supporting)
Shinichi Hashimoto (Investigation: Equal)
Takeshi Shimaoka (Resources: Equal)
Noriko Tabata (Methodology: Equal)
Miho Watanabe-Takahashi (Resources: Supporting)
Kiyotaka Nishikawa (Resources: Supporting)
Hiroshi Yanagawa (Data curation: Supporting)
Motoharu Seiki (Conceptualization: Supporting)
Kouji Matsushima (Conceptualization: Supporting)
Taro Yamashita (Data curation: Supporting)
Shuichi Kaneko (Conceptualization: Supporting)
Masao Honda, PhD, MD (Conceptualization: Lead; Writing – original draft: Equal)

Conflicts of interest
The authors disclose no conflicts.

Funding
Supported by the Japan Agency for Medical Research and Development under grant numbers JP20fk0210073, JP20fk0210048, JP20fk0210034, JP20fk0210046, JP20fk0210081, JP20fk0310110, JP20fk0210049, and 18K07966.